

Macrophage Phosphoproteome Analysis Reveals MINCLE-dependent and -independent Mycobacterial Cord Factor Signaling

Authors

Madlen Hansen, Julian Peltier, Barbara Killy, Bushra Amin, Barbara Bodendorfer, Anetta Härtlova, Sebastian Uebel, Markus Bosmann, Jörg Hofmann, Christian Büttner, Arif B. Ekici, Mario Kuttke, Henrik Franzyk, Camilla Foged, Sandra Beer-Hammer, Gernot Schabbauer, Matthias Trost, and Roland Lang

Correspondence

roland.lang@uk-erlangen.de

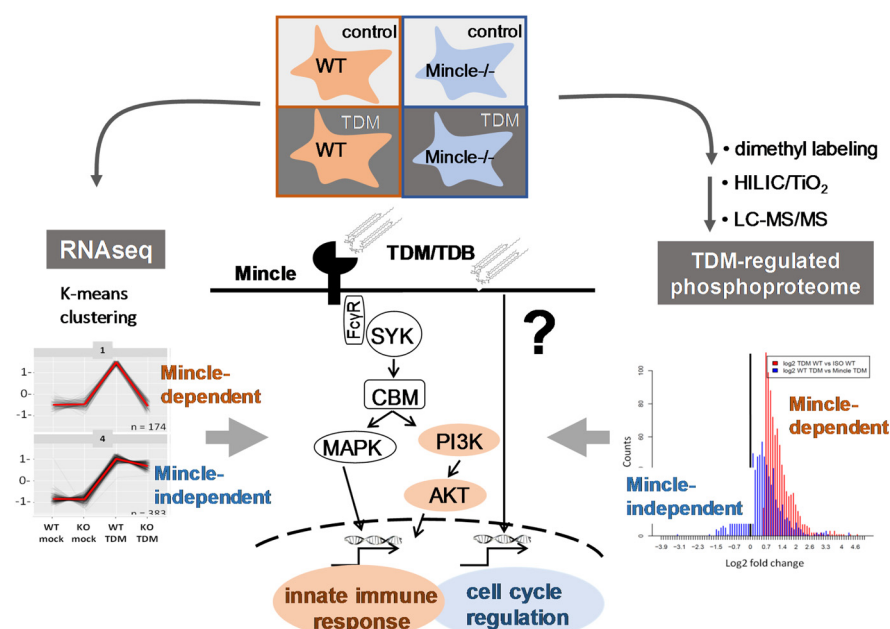
In Brief

First quantitative phosphoproteome analysis of TDM-activated macrophages reveals new insights in biological processes of macrophages stimulated with the mycobacterial cord factor. Surprisingly, the bioinformatic results revealed Mincle-dependent and -independent phosphorylation, which appear to affect different biological processes. Whereas PI3K/AKT signaling, dependent on Mincle, is involved in TDM-induced cytokine regulation, Mincle-independent phosphorylation and transcriptomic changes were linked to cell cycle regulation. Collectively, the observed reprogramming of macrophages by TDM might be relevant in the mycobacteria-macrophage interaction.



Highlights

- quantitative phosphoproteome analysis of TDM-activated macrophages.
- distinct Mincle-dependent and independent phosphorylation and gene regulations.
- Mincle-dependent activation of PI3K/AKT signaling by TDM.
- Mincle-independent macrophage response is linked to cell cycle regulation.

Graphical Abstract



Macrophage Phosphoproteome Analysis Reveals MINCLE-dependent and -independent Mycobacterial Cord Factor Signaling*[§]

Madlen Hansen[‡], Julian Peltier[§], Barbara Killy[‡], Bushra Amin[¶], Barbara Bodendorfer[‡], Anetta Härtlova[§], Sebastian Uebel[‡], Markus Bosmann^{||}, Jörg Hofmann[¶], Christian Büttner^{**}, Arif B. Ekici^{**}, Mario Kuttke^{§§}, Henrik Franzky^{¶¶},
 Camilla Foged^{||||}, Sandra Beer-Hammer^{‡‡}, Gernot Schabbauer^{§§}, Matthias Trost[§],
and  Roland Lang^{‡‡‡}

Immune sensing of *Mycobacterium tuberculosis* relies on recognition by macrophages. Mycobacterial cord factor, trehalose-6,6'-dimycolate (TDM), is the most abundant cell wall glycolipid and binds to the C-type lectin receptor (CLR) MINCLE. To explore the kinase signaling linking the TDM-MINCLE interaction to gene expression, we employed quantitative phosphoproteome analysis. TDM caused up-regulation of 6.7% and suppressed 3.8% of the 14,000 phospho-sites identified on 3727 proteins. MINCLE-dependent phosphorylation was observed for canonical players of CLR signaling (e.g. PLC γ , PKC δ), and was enriched for PKC δ and GSK3 kinase motifs. MINCLE-dependent activation of the PI3K-AKT-GSK3 pathway contributed to inflammatory gene expression and required the PI3K regulatory subunit p85 α . Unexpectedly, a substantial fraction of TDM-induced phosphorylation was MINCLE-independent, a finding paralleled by transcriptome data. Bioinformatics analysis of both data sets concurred in the requirement for MINCLE for innate immune response pathways and processes. In contrast, MINCLE-independent phosphorylation and transcriptome responses were linked to cell cycle regulation. Collectively, our global analyses show substantial reprogramming of macrophages by TDM and reveal a dichotomy of MINCLE-dependent and -independent signaling linked to distinct biological responses. *Molecular & Cellular Proteomics* 18: 669–685, 2019. DOI: 10.1074/mcp.RA118.000929.

Macrophages play a dual role in tuberculosis, because they harbor the intracellular *Mycobacterium (M.) tuberculosis* in the

phagosome, but also initiate the successful immune response by production of chemokines and cytokines. Recognition of mycobacteria by macrophages depends on the presence of pattern recognition receptors of the Toll-like receptor (TLR)¹ and C-type lectin receptor (CLR) families, and their interaction with mycobacterial ligands derived from the cell wall or mycobacterial nucleic acids. TLR2 recognizes the 19 kDa lipoprotein and Lipoarabinomannan (LAM) (1), whereas TLR9 is activated by mycobacterial DNA containing unmethylated CpG motifs (2, 3). Several SYK-coupled activating CLR contribute to the macrophage response to mycobacteria, including Dectin-1 (4, 5), Dectin-2 binding manLAM (6), DCAR as a receptor for phosphatidyl-inositol mannosides (7), and MINCLE and MCL, which are receptors for the mycobacterial cord factor (8–11). The cord factor, trehalose-6,6'-dimycolate (TDM), is the major cell wall glycolipid and is enough to elicit several hallmarks of the mycobacteria-host interaction, i.e. inflammatory gene expression in macrophages, adjuvant activity toward Th1/Th17 responses, and granuloma formation *in vivo* (8, 12–14). TDM, and its synthetic glycolipid analog trehalose-6,6'-dibehenate (TDB), directly bind to MINCLE, and with lesser affinity to MCL (9). MINCLE-deficiency in macrophages and mice abrogates TDM-induced cytokine production, adjuvant activity and granuloma formation (8, 10, 15).

The transcriptional responses induced by ligation of TLR or CLR family members are overlapping, as may be expected based on their similarity in function as pattern recognition receptors, and include expression of pro-inflamma-

From the [‡]Institute of Clinical Microbiology, Immunology and Hygiene, Universitätsklinikum Erlangen, Friedrich-Alexander-Universität Erlangen-Nürnberg, Erlangen, Germany; [§]Institute for Cell and Molecular Biosciences, University of Newcastle, Newcastle, UK; [¶]Chair of Biochemistry, Department of Biology, Friedrich-Alexander-Universität Erlangen-Nürnberg, Erlangen, Germany; ^{||}Center for Thrombosis and Hemostasis, Universitätsmedizin Mainz, Germany; ^{**}Institute of Human Genetics, Friedrich-Alexander-Universität Erlangen-Nürnberg, Germany; ^{‡‡}Department of Pharmacology and Experimental Therapy and Interfaculty Center of Pharmacogenomics and Drug Research, University of Tübingen; ^{§§}Institute of Vascular Biology and Thrombosis Research, Medical University of Vienna, Vienna, Austria; ^{¶¶}Department of Drug Design and Pharmacology, Faculty of Health and Medical Sciences, University of Copenhagen, Denmark; ^{||||}Department of Pharmacy, Faculty of Health and Medical Sciences, University of Copenhagen, Denmark

Received June 25, 2018, and in revised form, December 9, 2018

Published, MCP Papers in Press, January 11, 2019, DOI 10.1074/mcp.RA118.000929

tory chemokines and cytokines. However, there are also distinct response patterns linked to specific biological responses (16). For example, the TLR9 ligand CpG DNA induces high level IL-12 production and thereby provides a strong signal for Th1 differentiation. In contrast, the CLR ligands Curdlan (via DECTIN-1) and TDB (via MINCLE) induce robust Th17-type CD4⁺ T cell responses through production of IL-1 β and IL-23 (10, 14, 15, 17). These distinct gene expression patterns of macrophages stimulated with ligands for either TLR or CLR can be attributed to the differences in signal transduction pathways between both receptor families. TLR signaling is dependent on the adapter protein MYD88 (engaged by all TLR except TLR3) and/or TRIF (engaged by TLR3 and TLR4), the kinases IRAK4 and TBK1, and the E3 ligase TRAF6, to activate the transcription factors NF- κ B and Interferon regulatory factors (IRF) (reviewed in (18)). TLR signaling has been intensely investigated in the last 15 years, including several proteomic and phosphoproteomic studies, revealing new kinases and signaling modules relevant for the transcriptional response to TLR ligands (19–21).

Activating CLR share signaling through an ITAM motif and the kinase SYK (22). Dectin-1 directly recruits SYK via a hemi-ITAM motif (23), whereas MCL, MINCLE and DECTIN-2 associate with the ITAM-containing FcR γ chain to activate SYK (16). Downstream of SYK, activation of PLC γ 2, phosphorylation of PKC δ (24), and assembly of the CARD9-BCL10-MALT1 complex is required for activation of NF- κ B (25). PLC γ 2 also triggers activation of the transcription factor NFAT and induces expression of EGR family members (26). However, in contrast to the TLR family, the signaling cascades downstream of SYK-coupled CLR have not been systematically studied using unbiased global proteomic and transcriptomic approaches.

Rapid signal transduction from pattern recognition receptors located at the cell membrane to the nucleus relies on multiple forms of post-translational modification (PTM) of proteins, altering the localization, interaction with other proteins, enzymatic activity or stability of the substrate proteins. Together with ubiquitination and acetylation, kinase-mediated phosphorylation is one of the best characterized molecular switches in cellular signaling (27). In CLR-induced macrophage activation, reversible phosphorylation regulated by kinases and phosphatases likely plays an essential role, as evidenced by the essential function of the kinases SYK and PKC δ , or the activation of the MAPK module, which lead to activation of transcription factors and thereby induce inflammatory gene expression. A comprehensive analysis of the changes in protein phosphorylation in response of macrophages to stimulation through a SYK-coupled CLR has not been reported yet. It is therefore unknown which kinases,

transcription factors and other signaling proteins in addition to the above-mentioned players are regulated by phosphorylation in response to CLR stimulation in macrophages.

Here, we investigated global phosphorylation of proteins in macrophages of wild type and MINCLE-deficient mice in response to stimulation with TDM to obtain new insight into the signaling and biological processes regulated through phosphorylation. To determine to which extent TDM-triggered protein phosphorylation is initiated through its receptor MINCLE, we compared TDM-stimulated wild type and Mincle-deficient macrophages. Although the phosphorylation of many canonical kinases in the SYK-CARD9 pathway was induced in a MINCLE-dependent manner, we observed a surprisingly large extent of MINCLE-independent protein phosphorylation. To investigate whether gene expression induced by TDM depends entirely on its receptor MINCLE, RNAseq analysis was performed. Consistent with the phosphoproteomic data, RNAseq analysis showed that a substantial fraction of the transcriptional response was at least partially independent of MINCLE. These MINCLE-independent changes in phosphorylation and gene expression were associated with cell cycle regulation and metabolic changes, whereas MINCLE was required for signaling and transcription programs linked to cytokine production and innate immune response. Because activation of the PI3K-AKT-GSK3 axis was MINCLE-dependent, we employed macrophages deficient in the PI3K regulatory subunit p85 α and observed a significant contribution of this pathway to the production of cytokines by cord factor-activated macrophages.

EXPERIMENTAL PROCEDURES

Mice and Macrophage Differentiation—C57BL/6 and *Mincle*^{−/−} mice (originally provided by the Consortium of Functional Glycomics) were bred at the animal facility of the Medical Faculty in Erlangen. PI3K p85 α -deficient mice (28) were provided by Dr. Gernot Schabbauer. *Msr1*^{−/−} mice were provided by Dr. Matthias Trost, *Fyb*^{−/−} mice by Dr. Annegret Reinhold, *C5aR1*^{−/−} mice by Dr. Markus Bosmann, and *p110 γ , δ* ^{−/−} mice (29) by Dr. Sandra Beer-Hammer. All mice were created on or backcrossed to a C57BL/6 background. Bone marrow cells were isolated and after erythrocyte lysis cultured in cDMEM supplemented with 10% FCS, 1% penicillin/streptomycin (Sigma Aldrich), 50 μ M β -mercaptoethanol and 10% (v/v) M-CSF containing L cell conditioned medium (LCCM) for 7 days. After overnight depletion of adherent cells, 5 to 6 \times 10⁶ of the nonadherent cells were seeded per 10 cm Petri dish. On day 3, 5 ml cDMEM + 10% LCCM were added, and differentiated bone marrow macrophages (BMM) were harvested on day 7.

Stimulation, Cell Lysis and Phosphopeptide Preparation—The glycolipid compounds TDM (Bioclot, Aidenbach, Germany) and TDB (Avanti Polar Lipids, Alabaster) were used in a plate-bound form. For coating onto tissue culture plates, TDM/TDB were dissolved in isopropanol (ISO) by incubation at 60 °C for several minutes and added to cell culture plates. ISO was evaporated by incubation at room temperature in a biological safety cabinet for several hours. TDM and TDB were used at 2 μ g/ml or 5 μ g/ml. Trehalose monoester (TMX) and diester (TDX) glycolipids containing C12 and C16 acyl chains were synthesized and purified as previously described (30) and coated for stimulation of macrophages at a concentration of 2 μ g/ml as

¹ The abbreviations used are: TLR, toll-like receptor; CLR, C-type lectin receptor; LAM, lipoarabinomannan; IRF, interferon regulatory factor; PTM, post-translational modification.

described above for TDM and TDB. Control ligands 0.5 μ M CpG ODN 1826 (TIB Molbiol, Berlin, Germany) and 20 ng/ml LPS (*Escherichia coli* 055:B5; Sigma Aldrich, Schnelldorf, Germany) were diluted in cDMEM. Overnight pre-stimulation of macrophages with 10 ng/ml LPS was performed in Petri dishes. The pharmacological AKT inhibitors Triciribine (5 μ M) and AKT-Inhibitor VIII (10 μ M; MERCK Millipore, Darmstadt, Germany) as well as the PI3K p110 isoform-specific inhibitors PIK-75 (1 μ M; Selleckchem) and TGX-221 (1 μ M; Selleckchem, Houston, TX) and the PI3K inhibitor LY294002 (20 μ M, EMD Millipore) were simultaneously added to the stimulation.

For phosphoproteome analysis 50×10^6 cells per sample were stimulated for 45 min. After washing cells with cold PBS, macrophages were harvested in PBS containing protease and phosphatase inhibitors (1:50 Roche Complete (50 \times); 1:50 NaF (0.5 M); 1:100 β -Glycerophosphat (1 M); 1:200 Na_3VO_4 (200 mM)). The samples were centrifuged for 5 min, 1400 rpm at 4 °C and the pellets were lysed with 100 to 200 μ l lysis buffer (1% Rapigest, 50 mM Tris pH8.0, 1 mM TCEP). Afterward, 1 μ l Benzamide was added.

pY Immunoprecipitation—After stimulation, cells were lysed with RIPA buffer containing proteinase and phosphatase inhibitors (Roche complete, 0.5 M sodium fluoride, 1 M β -glycerophosphate, 200 mM sodium orthovanadate). Cell lysates were sonicated and protein concentrations were assessed. Afterwards 500 μ g protein were incubated with Pure Proteome Protein G Magnetic Beads (MERCK Millipore) decorated with 4G10 anti-phospho Tyrosine antibody overnight. After removing the supernatant and washing the beads, the phosphoproteins on the beads were reduced with Dithiothreitol and alkylated with Iodoacetamide. The proteins were digested with Trypsin (Pierce). Supernatants were collected, centrifuged (20.000 \times g, 20 min, 4 °C), dried in the Speedvac and analyzed by LC-MS.

Experimental Design and Statistical Rationale—For the phosphoproteome analysis, we used LPS-primed macrophages from WT and MINCLE-deficient mice and stimulated them with plate-coated TDM or ISO solvent control for 45 min. Three completely independent experiments were performed for macrophage differentiation and stimulation, thus a sample size of three biological replicates was used. After cell lysis the proteins were reduced, alkylated and digested with trypsin. Then the peptide samples from experimental conditions to be directly compared (WT_TDM versus WT_ISO; and WT_TDM versus *Mincle*^{-/-}-TDM) were labeled with light or heavy formaldehyde and mixed together before further processing. Phosphopeptides were fractionated and enriched by HILIC and titanium-dioxide beads and analyzed by LC-MS/MS. Log₂ ratios of each protein/condition were calculated for the three independent experiments. Quantified mass spectrometry data was statistically analyzed using a two-tailed student's *t* test in Perseus v1.5.1.1 (31) as data was normally distributed. Phosphopeptides were considered significantly regulated if the following conditions were met: *p* < 0.05, |log₂(fold change)| > 0.58).

Mass Spectrometric Analysis—Protein amounts of lysates from three biological replicates of each WT and *Mincle*^{-/-} macrophages treated with plate-coated TDM or cultured in solvent-treated control wells (ISO) were determined by EZQ protein assay (Pierce). An equivalent of 4 mg of protein per replicate was reduced (10 mM TCEP, 30 min, 56 °C) and alkylated (10 mM Iodoacetamide, 30 min, at RT in dark) prior to trypsin digestion (Worthington, Lakewood, NJ, Trypsin TPCK treated) using a ratio 1:100 for 3 h and a second digestion with same ratio overnight. Peptides were desalted via C18Sep-Pak SPE (Waters) and dried under vacuum centrifugation.

Peptides samples were resuspended in 100 μ l of 100 mM TEAB and dimethyl labeled (32) as follows: WT-ISO and *Mincle*^{-/-}-TDM were labeled with the light isotope-coded chemicals (¹²CH₂O and NaBH₃CN) whereas the intermediate isotope-coded dimethyl chemicals (¹²CD₂O and NaBH₃CN) were used for the labeling of WT-TDM samples. The chemical reaction was quenched by the addition of 1%

ammonium hydroxide and further neutralized by the addition of 50% TFA. Labeled peptides were desalted via C18 Sep-Pak SPE (Waters Milford, MA) and dried under vacuum centrifugation and analyzed individually by LC-MS/MS to ensure > 95% labeling efficiency. The three different conditions were combined in 1:1 ratio as follows, WT-TDM (Intermediate) versus WT-ISO (light) and WT-TDM (intermediate) versus *Mincle*^{-/-}-TDM (light), and subjected to fractionation by hydrophilic interaction liquid chromatography (HILIC) (33). Peptides were collected in 13 fractions and subjected to phosphopeptide enrichment using TiO₂ spin columns before LC-MS/MS analysis (34–36).

Dimethyl-labeled samples were separated on an Ultimate 3000 Rapid Separation LC Systems chromatography (Thermo-Fisher Scientific, Waltham, MA) with a C18 PepMap, serving as a trapping column (2 cm \times 100 μ m ID, PepMap C18, 5 μ m particles, 100 Å pore size) followed by a 50 cm EASY-Spray column (50 cm \times 75 μ m ID, PepMap C18, 2 μ m particles, 100 Å pore size)(Thermo-Fisher Scientific) with a linear gradient consisting of 2.4–28% (ACN, 0.1% formic acid (FA)) over 120 min at 300 nl/min. Mass spectrometric identification was performed on an Orbitrap Fusion Tribrid mass spectrometer (Thermo-Fisher Scientific) operated in data-dependent, positive ion mode similar to previously published (35, 37). FullScan spectra were acquired in a range from 400 *m/z* to 1500 *m/z*, at a resolution of 120,000, with an automated gain control (AGC) of 300,000 ions and a maximum injection time of 50 ms. HCD fragmentation was performed at 33% collision energy for all included precursor ions and MS/MS fragments were detected in the linear ion trap mass analyzer in rapid mode.

Protein identification and quantification were performed using MaxQuant Version 1.5.3.17 (38) with the following parameters: stable modification carbamidomethyl (C); variable modifications phosphorylation (STY), oxidation (M), acetylation (protein N terminus), deamidation (NQ), hydroxyproline (P), quantitation labels Dimethyl and Dimethyl:2H4 on N-terminal and/or lysine, and trypsin as enzyme with 2 missed cleavages. Search was conducted using the Uniprot-Trembl Mouse database (55,505 entries, downloaded September 28th, 2015), including common contaminants. Mass accuracy was set to 4.5 ppm for precursor ions and 0.5 Da for ion trap MS/MS data. Identifications were filtered at a 1% false-discovery rate (FDR) at the protein level, accepting a minimum peptide length of 5 amino acids. Quantification of identified proteins referred to razor and unique peptides and required a minimum ratio count of 2. Dimethyl-based relative ratios were extracted for each protein/conditions and were used for downstream analyses.

Next Generation Sequencing—For RNAseq analysis 0.5×10^6 BMM were stimulated with 2 μ g/ml plate-coated TDM or evaporated isopropanol as solvent control for 24 h. Total RNA was then isolated using the PeqGold RNA Micro Kit (Peqlab Biotechnology GmbH, Erlangen, Germany) according to the manufacturer's guidelines. RNAs were stored at -80 °C and sent to the Next Generation Sequencing Core Unit of the University Hospital Erlangen for RNA sequencing. Quality and integrity of the isolated RNAs was confirmed by the Agilent 2100 Bioanalyzer (Agilent Technologies, Waldbrunn, Germany) with all RNAs having RIN > 8.5. RNAseq library preparation was done with pooled technical replicates using the TruSeq stranded mRNA Library Prep Kit (Illumina, Inc., San Diego, CA) and sequencing was performed on the Illumina HiSeq 2500 platform (100 bp single-end) (Illumina, Inc.). Trimmed sequencing reads were aligned to the *Mus musculus* reference genome GRCm38 using the RNA-seq aligner STAR (version 2.5.3a) (39). For gene level quantification the software package Salmon (40) was used. Data normalization (TMM, edgeR, Bioconductor R-package) and statistical analysis for identification of differentially expressed genes were performed using the limma Bioconductor R-package (41). Because of consistent sequencing depth

across all RNA samples, limma-trend was used for differential expression analysis. Based on a classical interaction model, differentially expressed genes were determined according to the following criteria: adjusted (Benjamini-Hochberg) p value < 0.05 , \log_2 fold-change > 1 . Gene ontology (GO) analyses were performed using Cytoscape BiNGO (Cytoscape version 3.5.1) (42) (Benjamini-Hochberg false discovery rate (FDR) correction p value < 0.05 and hypergeometric distribution). For pathway enrichment analysis the InnateDB (<http://www.innatedb.com>) analysis platform was used (Benjamini-Hochberg (FDR) correction p value < 0.05 and hypergeometric distribution).

Bioinformatic Analysis—Hierarchical clustering and visualization of regulated phosphopeptides in WT and *Mincle*^{−/−} macrophages by TDM was done in a heatmap and histogram using GProX Version 1.1.13, (43). To define sets of MINCLE-dependently and -independently regulated phosphorylation sites, the following parameters were used: MINCLE-dependent phosphorylation sites (TDM versus ISO: fold change ≥ 1.5 ; $p \leq 0.05$ and WT versus *Mincle*^{−/−} fold change ≥ 1.5) and MINCLE-independent phosphorylation sites (TDM versus ISO: fold change ≥ 1.5 ; $p \leq 0.05$ and WT versus, *Mincle*^{−/−} fold change ≤ 1.25).

GO and Pathway Analysis—Using innateDB (www.innateDB.com Version 5.4) the over-represented GO terms and pathways over the genomic background for MINCLE-dependent or -independent phosphorylation sites were analyzed (hypergeometric distribution and Benjamini-Hochberg FDR). Additionally, to compare TDM-induced phosphoproteins to a reference list containing all phosphoproteins detected in our experiment, the odds ratio ((number matches list A/number non-matches list A)/(number matches list B/number non-matches list B)) and Fisher's exact probability were calculated for each GO term and pathway. Only GO terms with at least 4 and pathways with at least 5 identified phosphoproteins were accepted. As cutoff an odds ratio ≥ 1.3 and a corrected p value ≤ 0.05 were used.

Kinase Motifs—Phosphorylation sites were analyzed for over-represented kinase motifs using motif-x (motif-x.med.harvard.edu, Version 1.2 10.05.06). MINCLE-dependent or independent phosphorylation sites were analyzed versus our own reference list containing all phosphorylation sites detected in at least 2 replicates (7436 peptides). The following parameters were used: width = 13; occurrences = 10; significance 0.002.

Western Blotting—For Western blot analysis, cellular lysates were prepared in RIPA buffer containing proteinase and phosphatase inhibitors (Roche complete, 0.5 M sodium fluoride, 1 M β -glycerophosphate, 200 mM sodium orthovanadate). Western blotting was performed by 12%-SDS-PAGE and wet-blotting. The following Abs were used: anti-pSYK (Tyr^{525/526}), anti-SYK, anti-pERK (Thr²⁰²/Tyr²⁰⁴), anti-ERK1/2, anti-pAKT (Thr³⁰⁸), anti-pAKT (Ser⁴⁷³), anti-AKT, anti-pGSK-3 (Ser⁹), anti-phospho-p38 (Thr¹⁸⁰/Tyr¹⁸²) and anti-p38 (Cell Signaling, Frankfurt, Germany), anti-Mincle (clone 4A9, MBL, Woburn, MA), anti-phospho-Tyrosine 4G10 (MERCK Millipore), anti- α -Tubulin (Sigma Aldrich) and anti-GRB2 (BD Biosciences, Heidelberg, Germany) as loading control and HRP-conjugated secondary Abs (Jackson Immuno Research Laboratories, Ely, UK).

qRT-PCR—Cellular lysates for quantitative RT-PCR were prepared with Trifast (Peqlab, Erlangen, Germany) to perform phenol/chloroform isolation according to manufacturer's protocol. cDNA synthesis was done using the High Capacity cDNA Reverse Transcription Kit (Applied Biosystems). For qRT-PCR primers and probes were selected from the Universal Probe library (Roche) and purchased from Metabion. Hprt was used as housekeeping control and fold changes were calculated by the $\Delta\Delta CT$ method.

Griess-assay and ELISA—Nitrite and cytokine concentrations were analyzed in the supernatant of 200,000 cells in 96-well plates (triplicates) after 48 h stimulation unless otherwise stated. Cytokine con-

centrations were determined by DuoSet Sandwich ELISA (R&D Systems, Wiesbaden, Germany) according to the manufacturer's protocol. NO production was assessed by measuring nitrite levels with the Griess assay. 10 ng/ml IFN γ (Peprotech, Hamburg, Germany) was used as costimulatory ligand for the Griess-assay.

Protein Concentration—To quantitate the protein content, 200,000 cells per well in 96-well plates (triplicates) were lysed with RIPA buffer containing proteinase and phosphatase inhibitors (see WB) and protein concentrations were assessed by BCA Protein Assay Kit (Thermo Fisher) according to the manufacturer's protocol.

MTT Conversion Assay—To quantitate macrophage content in the wells, a colorimetric assay measuring the activity of cellular NAD(P)H oxidoreductases as conversion of the tetrazolium dye MTT (3-(4,5-dimethylthiazol-2-yl)-2,5-diphenyltetrazolium bromide) was performed. MTT (20 μ l of a 5 mg/ml stock solution) was added to the cultures at the indicated time points. After 3 h of incubation at 37 °C, the formazan crystals formed were dissolved by addition of 150 μ l of a 10% SDS solution in HCl and incubation overnight. The OD_{570 nm} was then measured in an ELISA reader.

Statistical Analysis—Statistical analyses were performed using Prism5 (GraphPad Software). Significance was determined by unpaired Mann-Whitney test for non-Gaussian distribution. * $p \leq 0.5$, ** $p \leq 0.01$.

RESULTS

Kinetics and MINCLE-dependence of TDM/TDB-induced SYK/MAPK Activation and Cytokine Expression—MINCLE expression is low in resting macrophages but induced by TLR and CLR stimuli. To achieve robust MINCLE expression, enabling a synchronized signaling response to MINCLE triggering, we primed bone marrow-derived macrophages (BMM) over night with a relatively low dose of LPS (10 ng/ml). Stimulation with the cord factor trehalose-6,6'-dimycolate (TDM) or the synthetic glycolipid adjuvant trehalose-6,6'-dibehenate (TDB), both used in plate-coated form, triggered robust phosphorylation of SYK and of the MAPK ERK1/2 and p38, peaking between 40' and 120' after stimulation (Fig. 1A, 1B). Production of the cytokines G-CSF and TNF in response to TDM/TDB stimulation was detectable first after 120' (G-CSF) and 60' (TNF) (Fig. 1C, 1D). Confirming previous results (10, 45), kinase activation and cytokine production were almost completely MINCLE-dependent (Fig. 1). Activation of SYK and MAPK preceded expression and secretion of cytokines: between 40' to 60' after stimulation, we observed strong protein phosphorylation but no cytokine secretion. Thus, we decided to use this time window for unbiased phosphoproteome analysis, when changes in phosphorylation are likely directly induced by interaction of TDM with its receptor and not influenced by secondary effects of secreted cytokines.

Unbiased Detection of TDM-induced Protein Phosphorylation—Ligand binding by MINCLE leads to tyrosine phosphorylation of the kinases SYK and PKC δ (24, 45, 46). We therefore first used the antibody 4G10 to detect changes in tyrosine phosphorylation of proteins after macrophage stimulation by Western blotting, which revealed several differential bands in response to the MINCLE ligands TDB/TDM and the TLR9 ligand CpG ODN, respectively (supplemental Fig. S1A). Mass spectrometry analysis of 4G10-enriched immunopre-

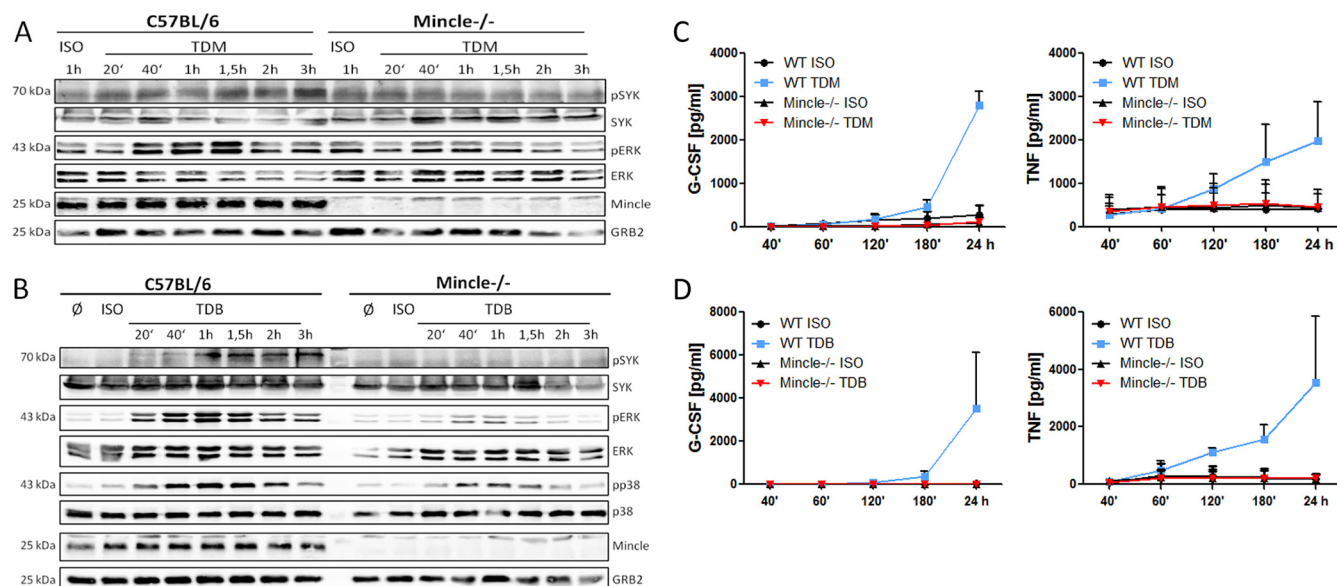


FIG. 1. TDM/TDB-induced kinase phosphorylation and cytokine expression. BMM from WT and *Mincle*^{-/-} mice were primed with LPS (10 ng/ml) over night, harvested and washed, and then transferred for stimulation to cell culture plates coated with 2 μ g/ml TDM (A, C), or 5 μ g/ml TDB (B, D), and isopropanol (ISO) as solvent control. Cells and supernatants were harvested at the indicated time points. (A; B) Phosphorylation of SYK, ERK and p38 was analyzed by Western blotting. (C; D) G-CSF and TNF were analyzed by ELISA. Mean \pm S.D. $n = 3$.

cipitation samples obtained 20' and 60' after stimulation with TDB was then used to identify tyrosine-phosphorylated proteins (supplemental Fig. S1B). A total of 42 tyrosine-phosphorylated proteins were detected in two independent experiments (supplemental Table S1), among them the established MINCLE-signaling protein PKC δ , the PI3K regulatory subunit 4 (Pik3r4, aka VPS15), and GSK-3, consistent with activation of the PI3K-AKT-GSK3 signaling pathway; the small GTPase RAB22a, shown to be recruited to phagosomes; and the cell cycle-associated proteins PRP4 and RBM14 (supplemental Fig. S1C).

Tyrosine phosphorylation constitutes only a small fraction of cellular protein phosphorylation, whereas phosphorylation of serine and threonine residues accounts for most protein kinase substrates. To globally detect protein phosphorylation on serine, threonine and tyrosine residues in a quantitative manner, we employed a protocol combining dimethyl labeling of cell lysates, enrichment of phosphopeptides by HILIC and titanium dioxide beads, and LC-MS/MS (Fig. 2A). In three independent experiments, we identified a total of 14173 phosphopeptides from 3727 phosphoproteins (Fig. 2B; supplemental Table S2). In accordance with previous work in LPS-stimulated BMM (21), most phosphorylated amino acids were serine (83%) and threonine (14%) residues, and only 3.4% of all sites were phospho-tyrosines (Fig. 2C). Treatment of WT macrophages with TDM significantly (1.5-fold, $p < 0.05$) up-regulated 846 (6.7%) and suppressed 484 (3.8%) of all phosphopeptides (Fig. 2D, left panel), whereas the comparison of WT and MINCLE-deficient TDM-stimulated macrophages showed 641 (5.5%) induced and 388 (3.4%) reduced phos-

phopeptides (Fig. 2D, right panel). Given the similar extent of regulation in these comparisons, we next determined whether TDM-induced regulation is MINCLE-dependent.

MINCLE-dependence of TDM-induced Protein Phosphorylation—The 1330 phosphopeptides significantly regulated by TDM in WT macrophages were analyzed by hierarchical clustering and visualized using a heatmap representation to determine whether up- or downregulation depended on MINCLE (Fig. 3A). For a large fraction of these phosphopeptides, regulation was similar in both comparisons, indicating that TDM-induced regulation was MINCLE-dependent (indicated by subgroups C1 and C5 in Fig. 3A). However, a substantial portion of TDM-regulated phosphopeptides did not differ between WT and MINCLE-deficient macrophages or were even regulated more strongly in the absence of MINCLE (subgroups C4 and C6 in Fig. 3A). Focusing on phosphopeptides induced by TDM-stimulation in WT macrophages, we used histogram plots to overlay the log₂-fold change distribution of WT versus MINCLE-deficient TDM-stimulated macrophages, which revealed that indeed around half of all phosphopeptides upregulated by TDM were not significantly more abundant in WT than in MINCLE-deficient macrophages (Fig. 3B). To analyze whether MINCLE-dependent and -independent kinase pathways may be linked to distinct cellular components and biological responses to TDM stimulation, we performed bioinformatic analyses using the InnateDB Gene Ontology and Pathway enrichment analysis tools (Fig. 3C, 3D; supplemental Table S3). Indeed, MINCLE-dependent phosphoproteins were associated with the GO terms "late endosome/lysosomal membrane," "endoplasmic reticulum," and

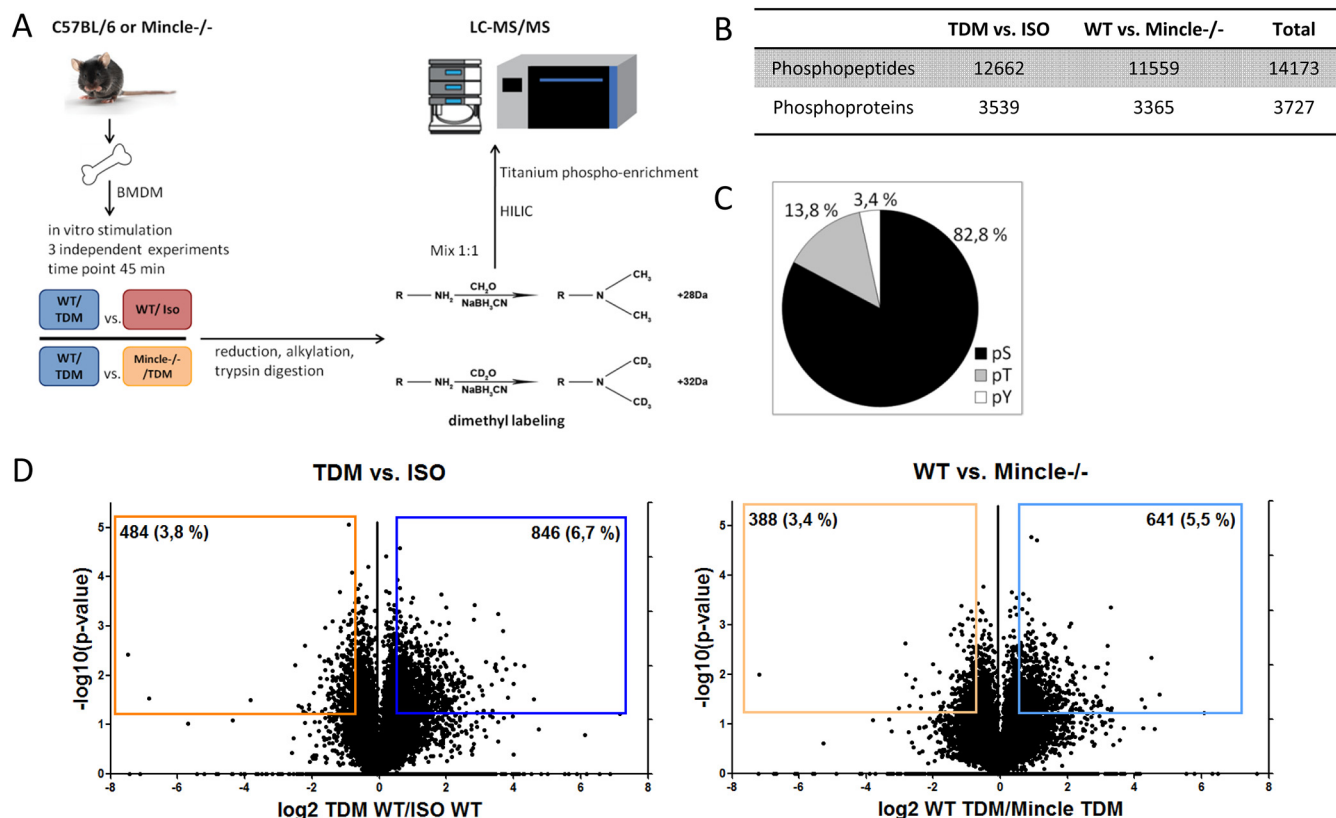


FIG. 2. Phosphoproteome analysis of macrophages stimulated with TDM. A, For the phosphoproteome analysis we used LPS-primed macrophages from WT and MINCLE-deficient mice and stimulated them with plate-coated TDM or ISO solvent control for 45 min. After cell lysis the proteins were reduced, alkylated and digested with trypsin. Then the peptide samples from experimental conditions to be directly compared were labeled with light or heavy formaldehyde and mixed together before further processing. Phosphopeptides were fractionated and enriched by HILIC and titanium-dioxide beads, and analyzed by LC-MS/MS. B, Total numbers of phosphopeptides and phosphoproteins identified. C, Relative frequencies of phosphorylated serine, threonine and tyrosine residues. D, Volcano plots showing phosphosite regulation by TDM treatment of WT macrophages (left panel) and comparison of TDM-treated WT and MINCLE-deficient macrophages (right panel). Significantly regulated phosphopeptides ($p < 0.05$, $|\log_2(\text{fold change})| > 0.58$) are indicated by orange and blue boxes.

“cytoskeleton,” “innate immune response,” and with signaling pathways controlled by the adapter protein FcR γ and by PLC, two canonical players of MINCLE-signaling through SYK. In contrast, Mincle-independent phosphoproteins were enriched for the cellular components “early endosomal membrane” and “nuclear membrane,” for the biological processes or pathway terms “RNA splicing,” “chromatin organization/remodeling” and “cell cycle.”

Next, we employed the algorithm motif-X to search for footprints of MINCLE-dependent and -independent kinase activation in the phosphopeptide data set. The sets of significantly induced phosphopeptides were analyzed for enrichment compared with a reference set of 7436 peptides detected in at least 2 experimental replicates (supplemental Fig. S2). Mincle-dependent phosphopeptides showed the strongest enrichment for a novel LxSP motif, which has not been associated with a putative mammalian kinase yet, but was recently reported as a candidate substrate motif for the CMV-encoded kinase pUL97 (47). The substrate motifs of PKA and of PKC δ , an established kinase in the MINCLE pathway linking

SYK to CARD9 phosphorylation (24), were enriched in the MINCLE-dependent set of phosphopeptides. In addition, a substrate motif for the kinase GSK-3, which was tyrosine-phosphorylated in response to TDB (supplemental Fig. S1), was also detected in the MINCLE-dependent phosphopeptide set. On the other hand, motif-X analysis of MINCLE-independently induced phosphopeptides yielded exclusively a motif for the DNA-damage kinases ATM/ATR, which was previously also found to be enriched in the phosphoproteome of macrophages activated through TLR4 by LPS (21).

A graphical overview of the phosphoproteome data set is provided in Fig. 4. First, we confirmed MINCLE-dependent phosphorylation of several established C-type lectin receptor signaling proteins, including the phospholipase PLC γ 2 and PKC δ , which are upstream of the CARD9-BCL10-MALT1 complex; activation of the MAPK signaling module with phosphorylation of MEKK1 (MAP3K1), and ERK1 (MAPK3) and ERK2 (MAPK1). Next, we identified the Src-family kinases LYN and FYN, as well as the tyrosine kinase FES, as Mincle-dependent TDM-activated phosphoproteins. The serine/thre-

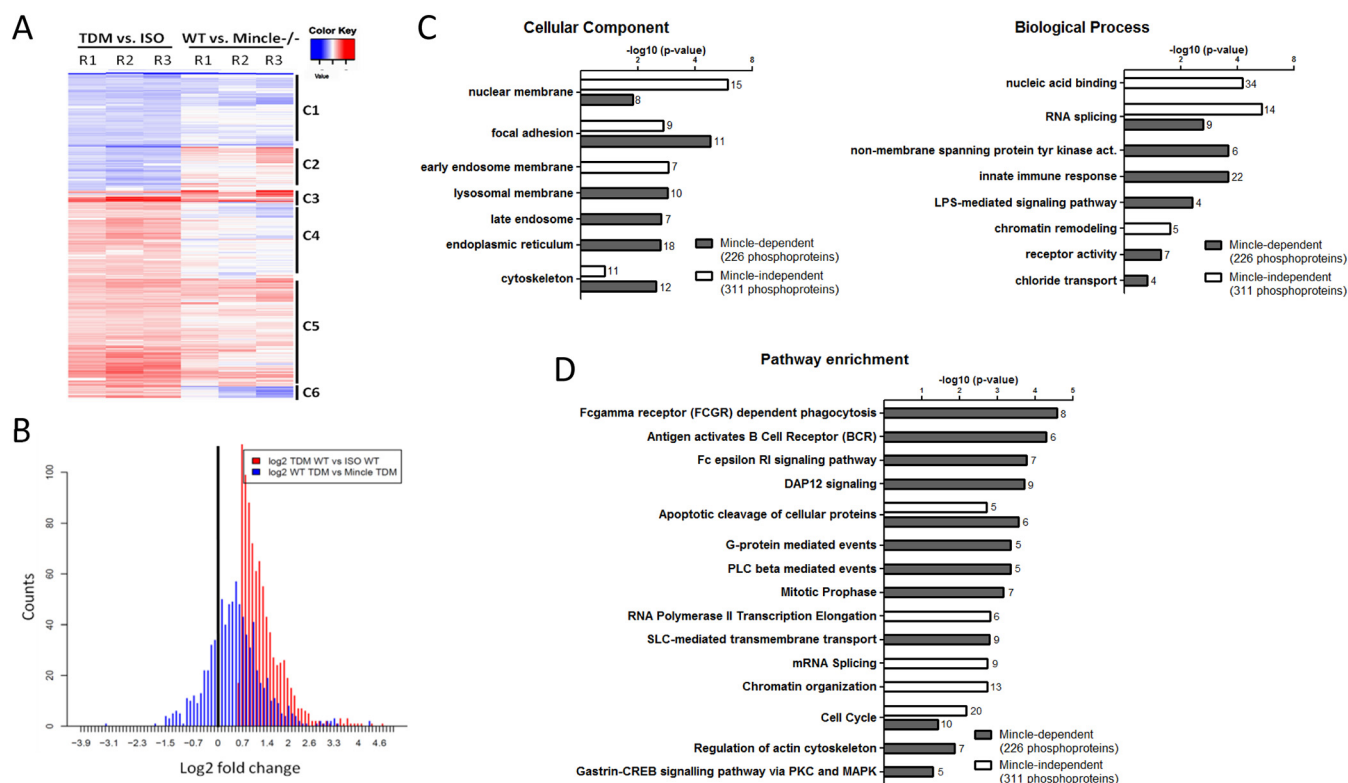


FIG. 3. Mincle-dependence of TDM-induced protein phosphorylation. A, Heatmap of regulated phosphopeptides WT and *Mincle*^{-/-} macrophages (significantly regulated in TDM versus ISO; $p < 0.05$). B, Histogram of TDM-upregulated phosphorylation sites in WT and *Mincle*^{-/-} macrophages (TDM versus ISO $fc > 1.5$ and $p < 0.05$). Red bars show distribution of fold changes for the TDM versus ISO comparison in WT macrophages; blue bars for the comparison WT versus MINCLE-deficient macrophages after stimulation with TDM. C, D, Bioinformatic analysis of MINCLE-dependent and -independent phosphoproteins using InnateDB. The MINCLE-dependent group was defined as TDM versus ISO $fc > 1.5$ $p < 0.05$ and WT versus *Mincle*^{-/-} $fc > 1.5$ (300 phosphorylation sites/226 phosphoproteins). The MINCLE-independent group was defined as TDM versus ISO $fc > 1.5$ $p < 0.05$ and WT versus *Mincle*^{-/-} $fc < 1.25$ (396 phosphorylation sites/311 phosphoproteins). C, GO term enrichment. D, Pathway enrichment analysis.

online kinase PRKD2, a downstream kinase mediating effects of PKC, has not been described in the Mincle-pathway yet. Several members of the NF- κ B signaling module were detected as phosphoproteins, including IKBKB (IKK β), IKBKG (NEMO), and the transcription factors NFKB2 (p100), NFKBIE (I- κ B ϵ) and NFKBIZ (I- κ B ζ). Although regulation of the phosphosites in these proteins did not pass our thresholds, a closer look at the data in [supplemental Table S2](#) indicated regulation of NF- κ B signaling by TDM: phosphorylation of the kinase IKK β at Ser-672 was reduced 1.43-fold ($p = 0.03$) and phosphorylation of the transcription factor NFKB2 at Ser-858 was increased 1.52-fold ($p = 0.09$). Consistent with the GO term enrichment of endosomal proteins, several transporters for chloride (CLCN3, CLCN7) and protons (ATP6V0A2, TCIRG1 (48)), the metalloredutase STEAP3 (49), and the endosomal GTPase RAB8A (50), were MINCLE-dependently phosphorylated in response to TDM, pointing to regulation of endosomal maturation and trafficking processes. The phosphorylation of 9 solute carrier proteins (SLC) suggests that MINCLE signaling may have a larger impact on the exchange of amino acids, sugars and other nutrients into and out of the cell, or between different macrophage compartments.

With regard to Mincle-independent phosphorylation, the adapter proteins DAB2 and FYB, the tyrosine kinase HCK and the focal adhesion kinase PTK2 may be involved in the phosphorylation of several cytoskeletal (MYOF, MARCKS), ribosomal (EIF4G1, EIF4H1) and nuclear proteins, such as LMNA and PCM1, the transcription factors ARNT and FOXN3, chromatin remodelers (MECP2, REST) and constituents of PML nuclear bodies (ATRX, SP100, SUMO1).

Interestingly, several cell surface receptors were phosphorylated in response to TDM stimulation (including the scavenger receptor MSR1, the complement receptor C5aR1, the chemokine receptor CXCR4, and the cation channel TRPV2, raising the possibility of parallel signaling pathways triggered by TDM stimulation, which may account for at least some of the MINCLE-independent phosphorylation events. Macrophages from several knockout mouse lines (*Msr1*^{-/-}, *Fyb*^{-/-}, *C5aR1*^{-/-}) were used to test whether these cell surface receptors and adapter proteins phosphorylated in response to TDM play an essential role for the signaling and cytokine production. No differences were observed in the extent of phosphorylation of SYK, AKT or ERK1/2, nor in the release of G-CSF, IL-6 or CCL2, in the absence of MSR1 ([supplemental](#)

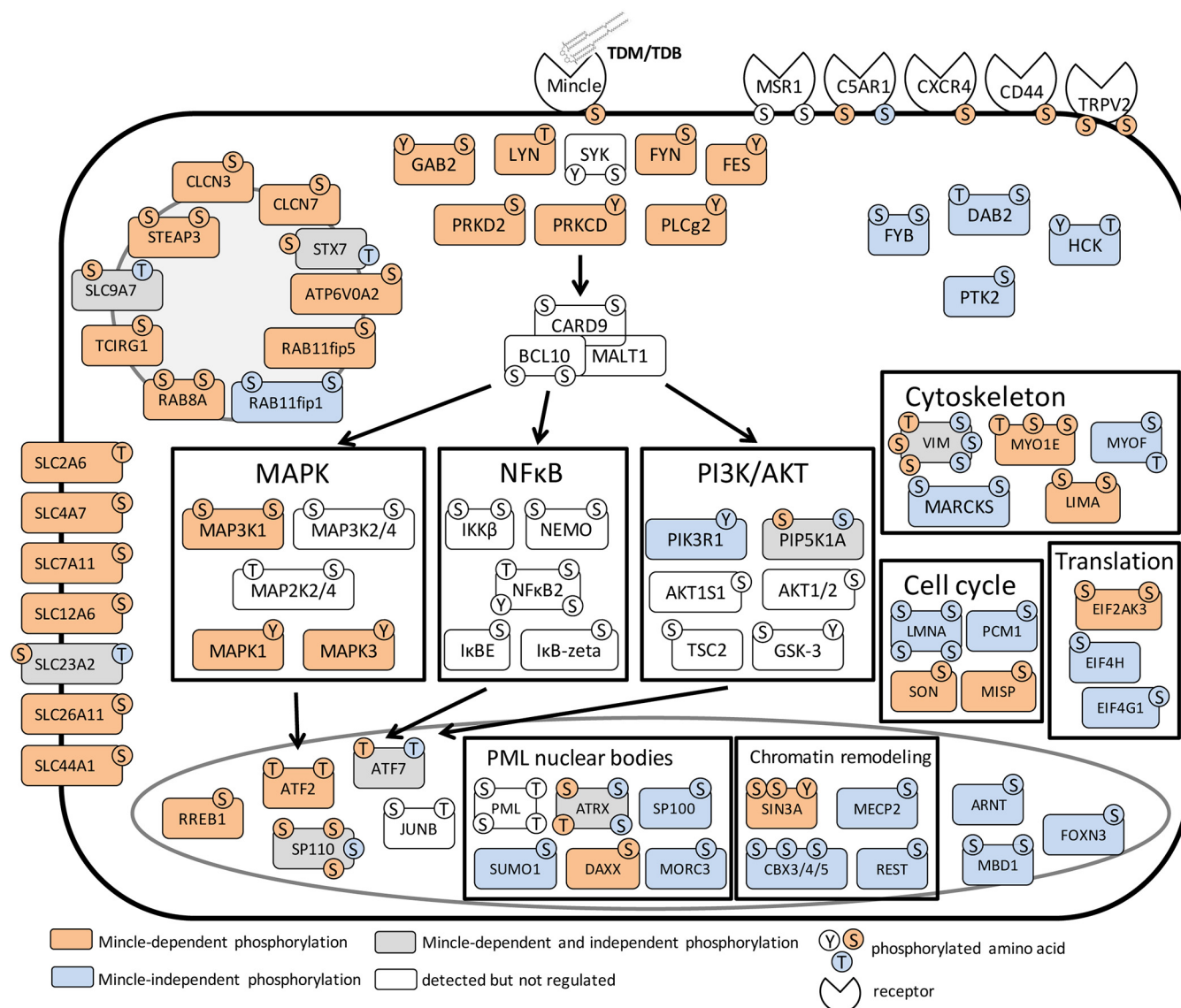


Fig. 4. Graphical overview of the phosphoproteome data set. Overview of MINCLE-dependently and -independently phosphorylated proteins after stimulation with TDM for 45 min. Summarized hotspots of TDM-induced phosphorylation at the level of pathways, biological processes and cellular components. Proteins depicted in orange are phosphorylated dependent on MINCLE whereas proteins depicted in blue are MINCLE-independently phosphorylated. The proteins depicted in gray have MINCLE-dependently and -independently regulated phosphorylation sites. The non-filled proteins could be detected in the phosphoproteome but they are not regulated by TDM.

Fig. S3A, S3B), C5aR1 (supplemental Fig. S4A, S4B) or the adapter FYB (supplemental Fig. S5A, S5B).

MINCLE-dependent Activation of PI3K-AKT Signaling by TDM—Several phosphoproteins associated with PI3K-AKT signaling were detected in the phospho-tyrosine and phosphoproteome data sets, including the regulatory PI3K subunit p85 α (PIK3R1), AKT1/2, and its substrates AKT1s, TSC2 and GSK-3 (Fig. 4; supplemental Fig. S1). Although AKT activation in response to TDB was recently reported (51), the canonical AKT phosphosites Thr³⁰⁸ and Ser⁴⁷³ were not detected in the proteomic data sets. We therefore analyzed AKT phosphorylation by immunoblot and observed that stimulation of LPS-primed macrophages with TDM and TDB, but not with the

TLR9 ligand CpG, induced robust phosphorylation of AKT at Thr³⁰⁸ and Ser⁴⁷³ (Fig. 5A), which correlates with AKT kinase activity. Phosphorylation of AKT started 40' after stimulation and was almost completely dependent on MINCLE (Fig. 5B). We next tested the functional importance of AKT activity by employing the inhibitors Triciribine and AKT-Inhibitor VIII, which both suppressed the production of G-CSF, whereas release of IL-6 and NO were not affected (Fig. 5C). Phosphorylation of AKT in response to TDM was completely abrogated by treatment with the PI3K inhibitor LY294002, which also inhibited G-CSF production (supplemental Fig. S6A–S6C). There are four isoforms of the class I PI3K catalytic subunit, of which p110 γ and p110 δ are mainly expressed in hematopoi-

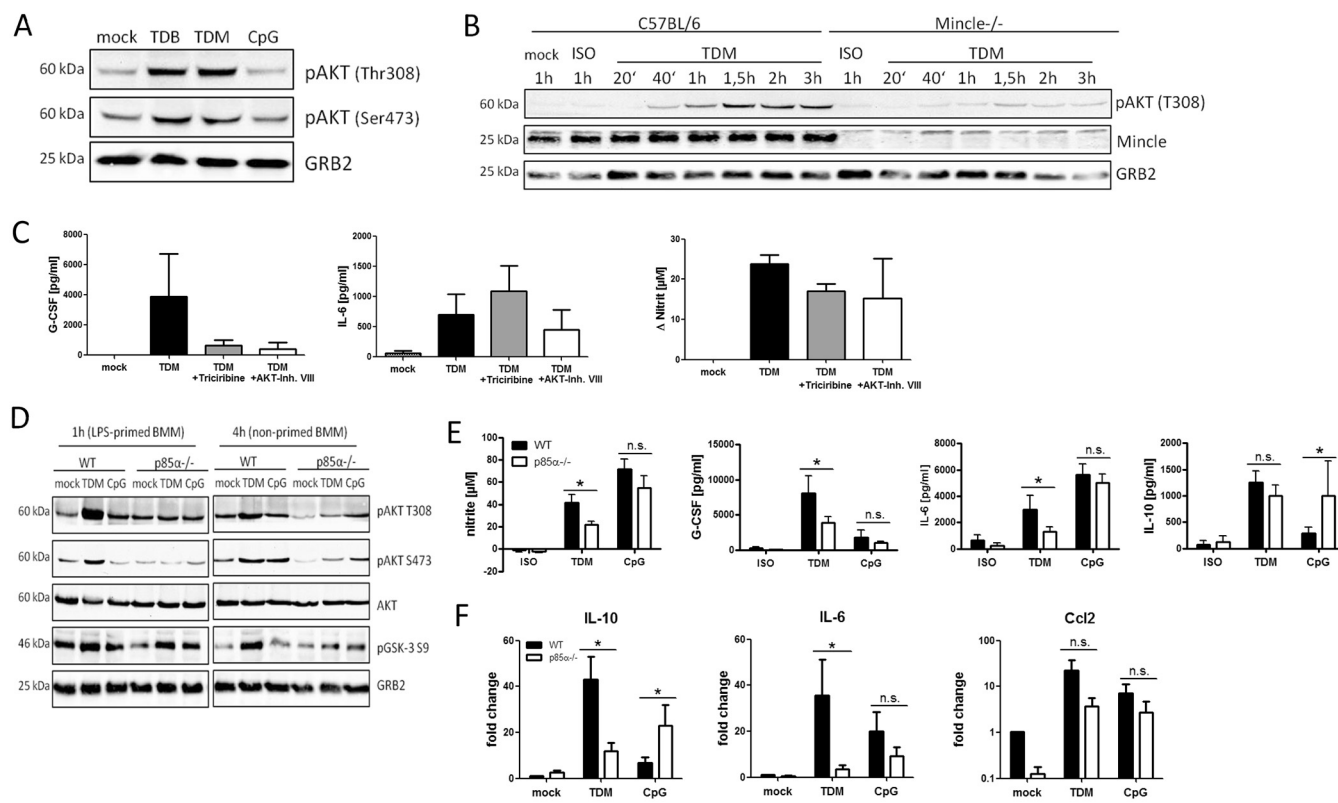


FIG. 5. Activation of PI3K-AKT signaling by TDM. A, Phosphorylation of AKT on T308 and S473 by TDM and TDB. Stimulation of LPS-primed BMM for 1h with TDM, TDB or CpG. B, Phosphorylation of AKT is MINCLE-dependent. Stimulation of LPS-primed BMM with TDM for indicated time points in C57BL/6 or *Mincl*^{-/-} mice. C, Cytokine production and NO release were analyzed from TDM-stimulated or non-stimulated BMM which are simultaneously treated with AKT inhibitor Triciribine or AKT Inhibitor VIII ($n = 3$). D, Reduced TDM-induced AKT phosphorylation in PI3K *p85α*^{-/-} BMM compared with WT. Analysis of AKT phosphorylation after 1 h stimulation with TDM or CpG in LPS-primed and after 4 h stimulation in non-LPS-primed WT and *p85α*^{-/-} macrophages. E, Reduced TDM-induced cytokine (48 h, +LPS) and NO (48 h, +IFN γ) levels in *p85α*^{-/-} BMM compared with WT (2 independent experiments with 2 mice each per genotype). (F) Gene expression analyzed by RT-qPCR of LPS-primed BMM stimulated with TDM or CpG for 24h. $n = 5$ mice pooled from 3 independent experiments. n.s. = not significant.

etic cells (52). Macrophages derived from *p110γ/δ* double-deficient mice responded with normal AKT phosphorylation and unaltered G-CSF production to TDM; in contrast, combined treatment with inhibitors specific for *p110α* and *p110β* (PIK-75 and TGX-221, resp.) prevented AKT phosphorylation and G-CSF release in WT and *p110γ/δ*-deficient macrophages (supplemental Fig. S6D, S6E), suggesting that *p110α* and/or *p110β* are the catalytic isoforms responsible for phosphorylation of AKT and expression of G-CSF. The catalytic subunits *p110α*, β , δ all associate with the regulatory subunit PIK3R1 (aka *p85α*) (supplemental Fig. S6F), which stabilizes them and contains an SH2 domain for interaction with tyrosine phosphorylated proteins (52). Therefore, we employed *p85α*^{-/-} macrophages as a genetic tool to probe the functional role of PI3K activation. In the absence of *p85α*, phosphorylation of AKT on Ser473 and on Thr308 was strongly reduced after TDM-stimulation of LPS-primed and of resting macrophages (Fig. 5D). Phosphorylation of the AKT substrate GSK-3 at Ser9 was also reduced in non-primed *p85α*^{-/-}

macrophages (Fig. 5D). These signaling defects were selective, because phosphorylation of SYK and ERK1/2 was unaltered (not shown). Production of NO, G-CSF and IL-6 were all significantly reduced in *p85α*^{-/-} macrophages (Fig. 5E). mRNA expression of IL-6, but not of CCL2, was strongly attenuated in response to TDM stimulation in *p85α*^{-/-} BMM; although the levels of IL-10 detected in the supernatant were not altered (Fig. 5E), *p85α*-deficient macrophages showed significantly reduced expression of IL-10 mRNA (Fig. 5F).

Transcriptome Analysis of Macrophage Activation by TDM Reveals MINCLE-dependent and -Independent Gene Expression—The unexpectedly prominent MINCLE-independent phosphorylation events prompted us to re-assess the notion that transcriptional activation of macrophages by TDM is entirely dependent on MINCLE-signaling via FcR γ -SYK-CARD9 (10, 45). WT and MINCLE-deficient macrophages stimulated for 24 h with TDM were analyzed by RNAseq using Illumina HiSeq. Hierarchical clustering of differentially expressed genes showed that resting WT and MINCLE-deficient

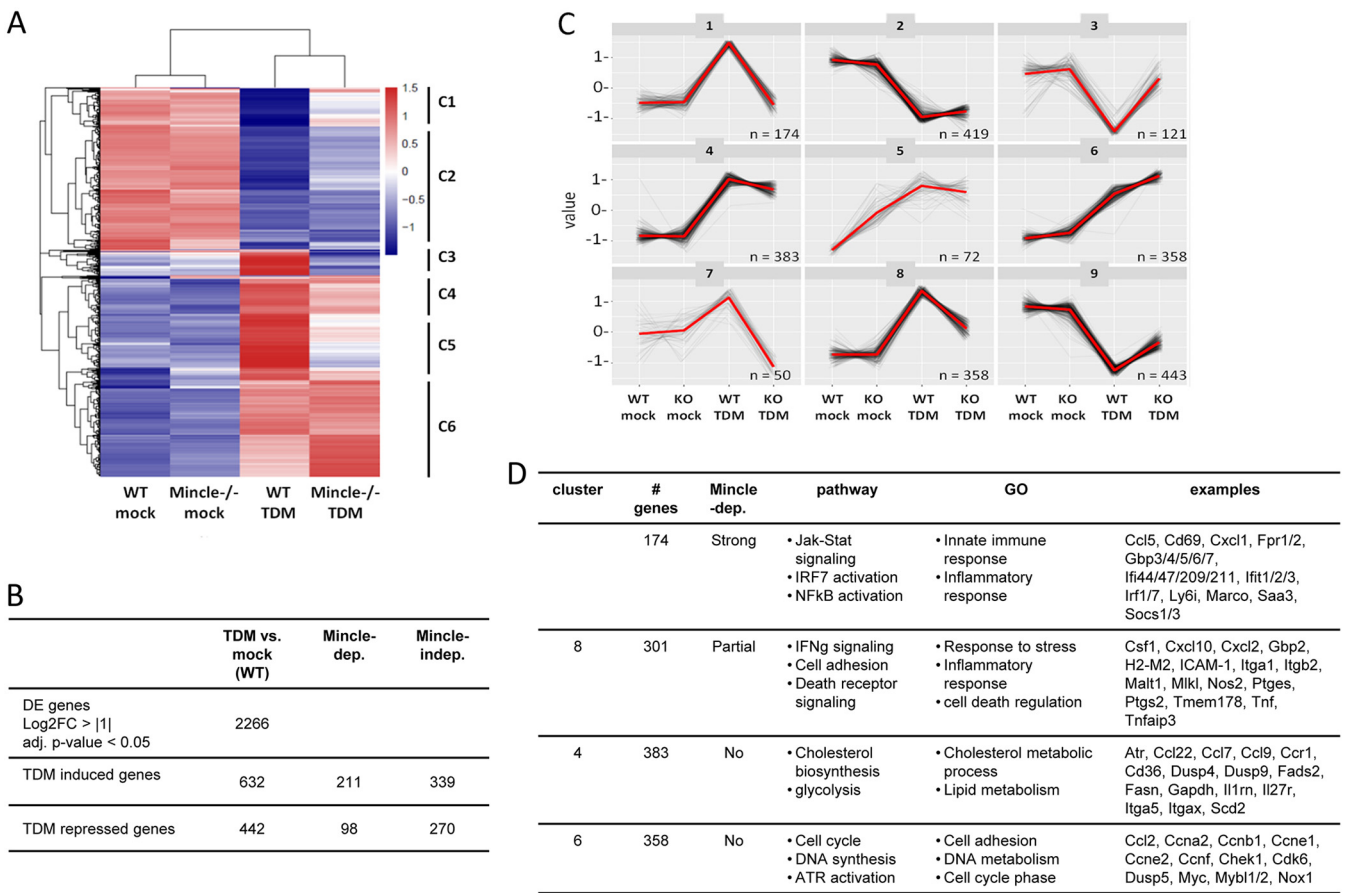


FIG. 6. RNAseq of TDM-induced macrophage activation. *A*, Hierarchical clustering of differentially expressed genes. *B*, Numbers of differentially expressed genes: TDM-induced genes ($\text{Log}_2\text{FC} (\text{Wt_TDM}/\text{Wt_mock}) > 1.58$, adj. p value < 0.05), TDM-repressed genes ($\text{Log}_2\text{FC} (\text{Wt_TDM}/\text{Wt_mock}) < -1.58$, adj. p value < 0.05); MINCLE-dependent: $\text{Log}_2\text{FC} (\text{Wt_TDM}/\text{Mincle}^{-/-}\text{-TDM}) > 1.5 / < -1.5$, and MINCLE-independent: $\text{Log}_2\text{FC} (\text{Wt_TDM}/\text{Mincle}^{-/-}\text{-TDM}) < 1 / > -1$. *C*, K-means clustering showing separation in MINCLE-dependent and -independent TDM target genes. *D*, selected GO and pathway terms enriched in different clusters.

macrophages clustered closely together. Stimulation with TDM caused substantial up- and downregulation of gene expression in WT macrophages, with subclusters of apparently MINCLE-dependent and -independent gene expression (Fig. 6A). This impression was confirmed by applying fold change filtering, with 211 clearly MINCLE-dependent and 339 -independent TDM-induced genes (Fig. 6B). K-means clustering of TDM-regulated genes (supplemental Table S4) was then used (Fig. 6C) to define gene sets with a characteristic pattern of induction and MINCLE-dependence for further bioinformatics analysis (Fig. 6D, supplemental Table S5 and S6). Clusters 1 and 8 contained the largely or partially MINCLE-dependently induced TDM target genes, which were enriched for pathway annotations of Interferon signaling, TLR- and NF- κ B-signaling, and innate immune response. In contrast, MINCLE-independent gene expression (clusters 4 and 6) were associated with metabolic alterations (cholesterol biosynthesis, glycolysis, metabolism of lipids) and cell cycle regulation, respectively (Fig. 6C, 6D). Cluster 6 was also associated with “ATR activation,” consistent with the enrichment of

the ATM/ATR kinase motif found in the set of phosphopeptides upregulated in a MINCLE-independent fashion by TDM (supplemental Fig. S2). Together, the RNAseq data set revealed a similar degree of MINCLE-independent responses as observed in the phosphoproteome data set, supporting the notion that not all TDM-triggered signaling is caused by binding to MINCLE. Moreover, although the transcriptomic and phosphoproteome data set cannot be compared directly, bioinformatics analysis yielded a concordant enrichment of terms associated with innate immune response for the MINCLE-dependent changes at the level of transcription and phosphoproteins. In contrast, the MINCLE-independent responses in both data sets were enriched for annotations linked to cell cycle regulation.

The MINCLE-independent TDM-induced Expression Program Is Also Upregulated by Trehalose Ester Glycolipids Not Binding to Mincle—To validate the findings from the RNAseq data set, qRT-PCR analysis of samples from independent experiments was performed. As expected, induction of mRNA expression for G-CSF and iNOS (belonging to the MINCLE-

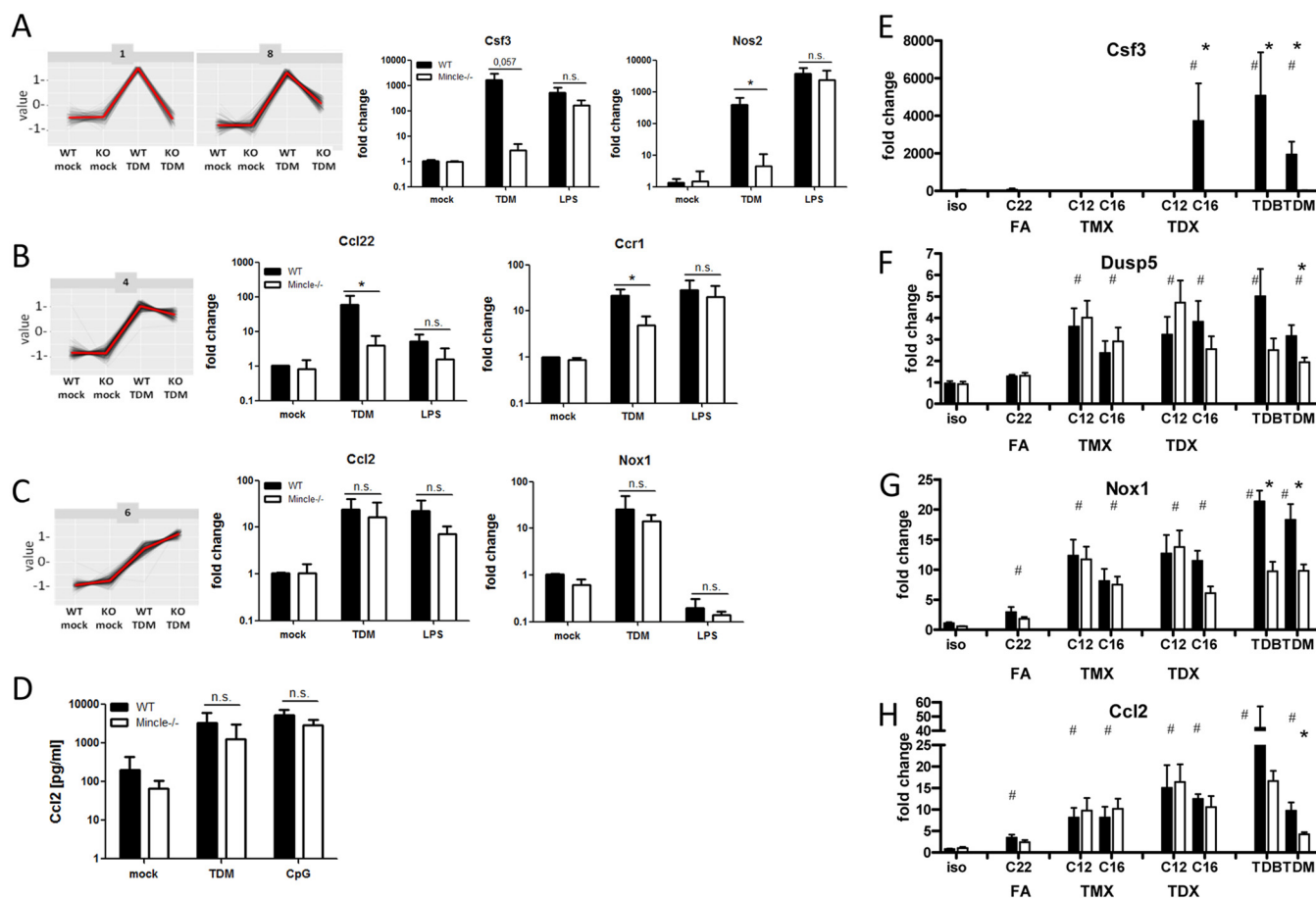


FIG. 7. Validation RNAseq data for MINCLE-dependent and -independent gene expression. A–C, WT and *Mincle*^{-/-} BMM were stimulated with TDM or CpG for 24h and gene expression was analyzed by qRT-PCR. A, *Csf3* and *Nos2* (MINCLE-dependent clusters 1 and 8). B, *Ccl22* and *Ccr1* from cluster 4. C, *Ccl2* and *Nox1* from cluster 6. *n* = 4 from 2 independent experiments. D, CCL2 protein in supernatants of macrophages stimulated for 48 h. Mean ± S.D. *n* = 5 from 3 independent experiments. n.s. = not significant. E–H, Induction of gene expression by trehalose monoesters (TMX) and diesters (TDX) with C12 and C16 acyl chains, and by the fatty acid (FA) behenate (C22). E, *Csf3*, F, *Dusp5*, G, *Nox1*, H, *Ccl2*. Mean and S.E., *n* = 5–6 mice, pooled from 3 independent experiments. * *p* < 0.05 WT versus *Mincle*^{-/-}; # *p* < 0.05 treatment versus mock in WT BMM. All other responses to identical stimuli were not significantly different between WT and *Mincle*^{-/-} BMM.

dependent clusters 1 and 8) was largely dependent on MINCLE (Fig. 7A). In contrast, the expression of the chemokine CCL22 and the chemokine receptor CCR1 (both contained in cluster 4) was partially (Fig. 7B), and of CCL2 and the NADPH oxidase NOX1 (two cluster 6 genes) was largely MINCLE-independent (Fig. 7C, 7D). To determine whether the MINCLE-independent response to TDM is indeed specific for the cord factor or can be caused more broadly by (glyco-)lipids, we tested a set of trehalose monoester (TMX) and diesters (TDX) with acyl chains of various length (C12 and C16). In previous work, we had observed that the trehalose diester form of C16 bound to MINCLE and triggered cytokine production from macrophages (53). Confirming our previous results, the trehalose diester of C16 (and TDM and TDB) strongly stimulated expression of *Csf3* in a completely *Mincle*-dependent manner, whereas the C22 behenic acid alone, the C12 trehalose diester, and the C12 and C16 monoesters did

not trigger *Csf3* mRNA expression (Fig. 7E) or G-CSF secretion (not shown). In contrast, the expression of the MINCLE-independent TDM-target genes *Dusp5*, *Nox1*, and *Ccl2* was significantly upregulated not only by the MINCLE-ligands (TDM, TDB, trehalose diester of C16), but also by the C12 diester and the C12 and C16 monoesters, whereas behenic acid coating of the plates alone only weakly induced expression of these genes (Fig. 7F–7H). Upregulation of *Dusp5*, *Nox1* and *Ccl2* was largely independent of MINCLE, with a partial reduction after TDM stimulation.

The Mincle-independent Response to TDM and Related Glycolipids Is Linked to Macrophage Survival Or Proliferation—Because GO and pathway enrichment analysis revealed that cluster 6 was enriched for “cell cycle” and “DNA synthesis,” we validated the expression of the cluster 6 genes *Myc*, *Ccne1*, *Ccne2*, and *Chek1* by qRT-PCR and confirmed their MINCLE-independent induction after TDM stimulation (Fig.

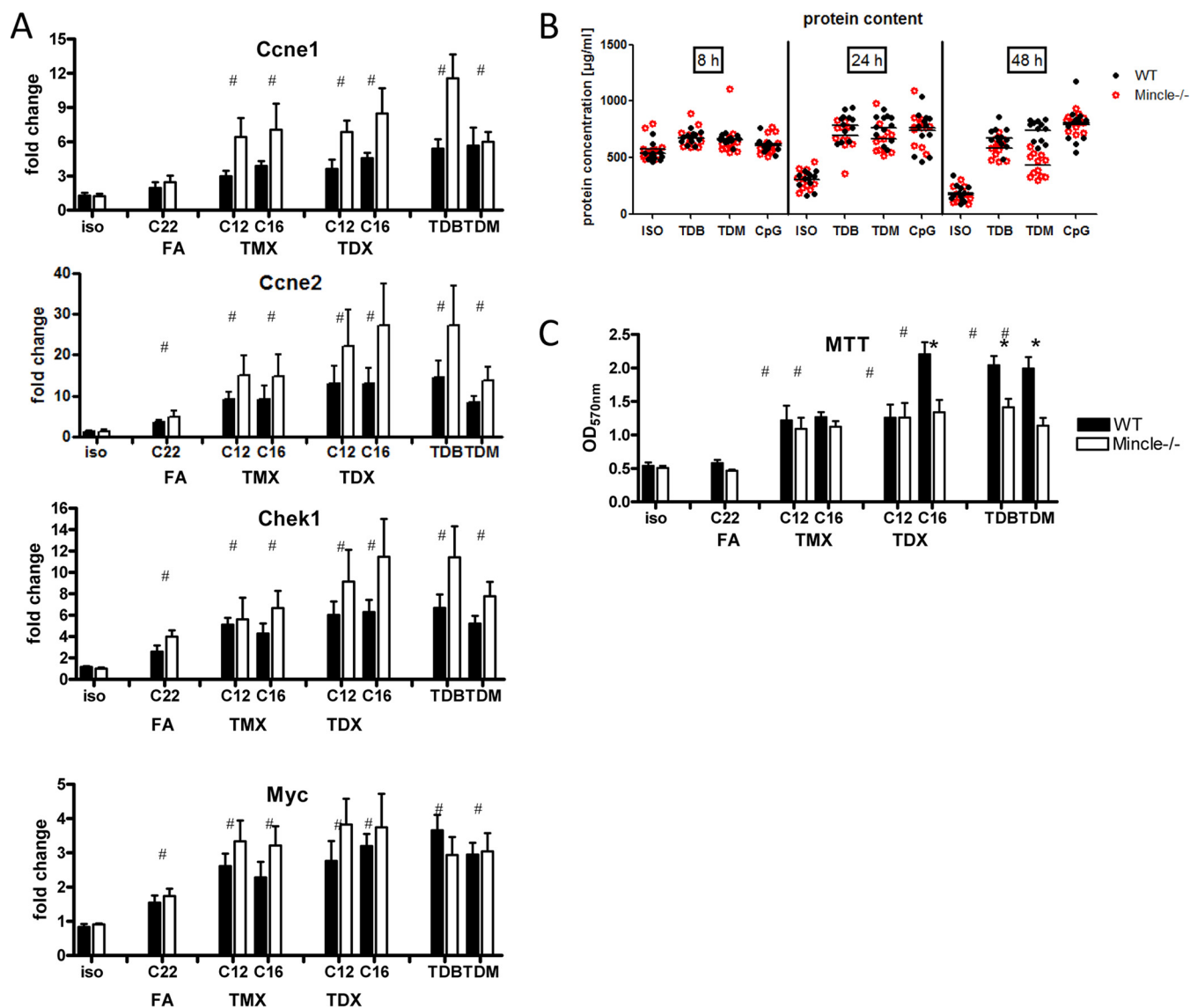


FIG. 8. Cell cycle-associated gene expression is MINCLE-independent. A, WT and *Mincle*^{-/-} BMM were stimulated for 24 h as indicated with TDM, TDB, the trehalose monoesters (TMX) and diesters (TDX) with C12 and C16 acyl chains, and the fatty acid (FA) behenate (C22). Gene expression of *Ccne1*, *Ccne2*, *Chek1* and *Myc* was then analyzed by qRT-PCR. Mean and S.E., $n = 5-6$ mice, pooled from 3 independent experiments. * $p < 0.05$ WT versus *Mincle*^{-/-}; # $p < 0.05$ treatment versus mock in WT BMM. All other responses to identical stimuli were not significantly different between WT and *Mincle*^{-/-} BMM. B, BCA assay for analysis of cellular protein content in BMM cultures stimulated for the indicated times with TDM, TDB or CpG ODN 1826. Pooled from four experiments. C, MTT conversion assay from BMM stimulated for 48h. Mean and S.E., $n = 5-6$ mice, pooled from 3 independent experiments. * $p < 0.05$ WT versus *Mincle*^{-/-}; # $p < 0.05$ treatment versus mock in WT BMM.

8A). As observed for DUSP5, CCL2 and NOX1 (Fig. 7E–7G), expression of these cell cycle-associated genes was not only upregulated in a MINCLE-independent manner by the cord factor, but to a similar extent also by synthetic trehalose diesters and monoesters of C12 and C16 fatty acids, and more weakly by behenic acid alone (Fig. 8A). *Ccne1* and *Ccne2* encode the cyclins E1 and E2, whose expression peaks in mid-G1 to early S-phase of the cell cycle (54). The proto-oncogene *Myc* encodes the E-box transcription factor MYC which is associated with proliferation and self-renewal

of macrophages (55, 56). CHEK1 is activated by the DNA-damage response kinase ATR and contributes to p53-dependent responses (57). We observed that macrophage cultures treated with TDM appeared much denser than control cells cultured in medium alone (supplemental Fig. S7A). This effect was also observed with the trehalose monoester and diester glycolipids, and appeared to be partially MINCLE-independent (supplemental Fig. S7A). This impression was quantitatively confirmed by measuring the protein content of the macrophage cultures (Fig. 8B). Of note, when analyzed

over time, the protein content of control cultures diminished, but stayed constant in the TDM-treated samples, suggesting that TDM prevented a loss of macrophages during starvation from growth factors, which was partially MINCLE-dependent after 48 h (Fig. 8B). Interestingly, the MINCLE-ligand glycolipids (TDM, TDB and the trehalose diester of C16) lead to a stronger enhancement of cellular protein content in the wells than the monoesters, and this difference was MINCLE-dependent (supplemental Fig. S7B). As an additional method to quantitate effects of TDM on macrophage survival and proliferation, we employed the MTT conversion assay. First, the effect of TDM and TDB was comparable to the activity of the macrophage growth factor M-CSF (supplemental Fig. S7C). MTT conversion after 48 h was significantly increased by all glycolipids, but not by behenic acid, with the strongest effect observed for the MINCLE ligands (TDM, TDB and the trehalose diester of C16) (Fig. 8C). Similar to the changes in total protein content, the MTT conversion rates of the untreated macrophages decreased over time (see 24 h time point in supplemental Fig. S7D), suggesting that the glycolipids caused increased survival of macrophages through the MINCLE-independent upregulation of cell cycle-associated genes after 24 h and additional MINCLE-dependent effects at the later 48h time point (Fig. 8B, 8C).

DISCUSSION

Recognition of the mycobacterial cord factor TDM by the CLR Mincle and the key role of SYK-CARD9-BCL10-MALT1 signaling has been firmly established by genetic deletion in mice. Compared with the well-studied TLR signaling pathways, an unbiased analysis of the signaling and transcriptome response to activation of MINCLE, or of related SYK-coupled CLR, is missing. This manuscript provides the first global assessment of macrophage activation by the mycobacterial cord factor TDM at the phosphoproteome level, combined with a corresponding RNAseq-based transcriptomic data set. Our results show substantial regulation of phosphopeptides in response to TDM, which was comparable in breadth with similar studies investigating the phosphoproteome of TLR-activated macrophages (21). We consider most of the changes in phosphopeptide abundance as a direct consequence of TDM-induced signaling, because at the early time point of 45 min after stimulation no secreted cytokines could be detected in the supernatant. Importantly, the comparison of WT and MINCLE-deficient macrophages in phosphoproteome and transcriptomic analysis allowed us to confirm the importance of the TDM-Mincle interaction, yet it also revealed an unexpectedly large fraction of MINCLE-independent changes, which are functionally separate from the Mincle-dependent responses.

MINCLE-dependent phosphorylation included several canonical players of this pathway, such as PKC δ and PLC γ 2, which was consistent with the enrichment of PKC δ kinase motifs among the phosphopeptides induced by TDM in a

MINCLE-dependent fashion. Because PKC δ is required for formation of the CBM complex and subsequent activation of NF- κ B (24), the strong enrichment of the pathway term “NF- κ B activation” and the GO category “inflammatory response” among the cluster of MINCLE-dependent TDM target genes in our RNAseq data fits very well.

Several Src-family kinases were activated by TDM-MINCLE, including FYN and LYN. Of interest in this context, LYN was very recently reported to directly interact with MINCLE after TDM stimulation and to attenuate its signaling by recruitment of SIRP1a and SHP1 (58). The signaling via the Src kinase LYN was triggered by MINCLE-dependent activation of the integrin CD11b (58); thus, the detection of induced LYN phosphorylation in our data set may indicate integrin activation as a regulatory pathway of the response to TDM.

Triggering of PI3K-AKT signaling by mycobacterial cord factor or its synthetic analog has recently been described in human DC (51) and in human neutrophil-like HL-60 cells (59). Although we detected phosphorylation of several PI3K-AKT-associated proteins, including AKT1/2 and the regulatory PI3K subunit p85, the canonical phosphopeptides indicating activated AKT (Thr³⁰⁸ and Ser⁴⁷³) were not found in the phosphoproteome data set, but readily detected as upregulated by TDB/TDM using immunoblot analysis. Our further data on the role of the PI3K/AKT pathway in TDM-induced macrophage activation indicate that the PI3K catalytic subunit isoforms p110 γ and p110 δ are redundant in macrophages, whereas pharmacological inhibition of p110 α and p110 β was enough to completely block AKT phosphorylation and TDM-induced G-CSF and IL-6 production. Although the lack of a phenotype in p110 γ/δ -deficient macrophages was at first surprising, given reports that p110 δ is the main isoform activated by tyrosine-kinase linked receptors in T cells and innate immune cells (60), these findings are concordant with previous reports showing redundancy between different p110 isoforms (61) and demonstrating a function for p110 β in macrophages (62). The regulatory PI3K subunit p85 α binds p110 α , p110 β and p110 δ and therefore appears to play a broader role in PI3K activation (52). Indeed, our data obtained with p85 $\alpha^{-/-}$ macrophages showed a strong reduction of TDM-induced phosphorylation of AKT and of several cytokines (Fig. 5). Strongly attenuated phosphorylation of AKT in the absence of p85 α was found previously in murine peritoneal macrophages stimulated with LPS (63) but has not been demonstrated after stimulation with a CLR ligand before. In contrast to earlier reports showing a selective reduction of the anti-inflammatory IL-10 and reciprocal overproduction of IL-12 by p85 $\alpha^{-/-}$ DC after stimulation with LPS (28), in our system both pro- and anti-inflammatory responses were similarly affected by p85 α deficiency (and by pharmacological inhibition of PI3K catalytic subunits p110 α and p110 β). Of note, Luyendyk *et al.* observed increased IL-6 and TNF production by p85 α -deficient peritoneal macrophages stimulated with LPS (63). At present we do not know whether this discrepancy reflects a differen-

tial role of p85-PI3K signaling in macrophages *versus* DC, or rather points to differences in the regulation of TLR- and CLR-driven responses by PI3K.

The functional annotation of Mincle-dependently regulated phosphoproteins showed strong enrichment for endo-/lysosomal and transport proteins (Figs. 3, 4), an effect we had not observed in our analysis of LPS-induced phosphoproteins (21). The strong phosphorylation observed for many solute carrier proteins may reflect ongoing signaling at the plasma membrane when macrophages are stimulated with plate-bound TDM as used here, whereas soluble ligands such as LPS could result in more rapid internalization and diversion of signalosomes to intracellular compartments. On the other hand, the strong MINCLE-dependent phosphorylation of phagolysosomal proteins is of interest regarding the intracellular mycobacterial life-style. Several of these phosphoproteins control phagosomal maturation or trafficking processes, suggesting that TDM-MINCLE signaling modulates the fate of the mycobacterial niche in macrophages. In fact, the proton pump TCIRG1 (*alias* ATP6V0A3) is important for acidification of the mycobacterial phagolysosome (48, 64). The metallo-reductase STEAP3 controls iron homeostasis in macrophages (49) but has not been implicated in the mycobacteria-macrophage interaction yet. The endosomal GTPase RAB8A recruits PI3K to regulate the signaling from endosomal TLRs (50), which is of special interest regarding the activation of PI3K-AKT signaling by TDM discussed above.

The robust MINCLE-independent kinase activation and transcriptional changes was a surprising result of our unbiased approach to macrophage reprogramming by the cord factor, given the strong MINCLE-dependence of TDM-induced inflammatory responses and adjuvant activity reported by us and others before (8, 10, 65). The availability of synthetic mono- and diesters of trehalose with fatty acids of various length (C12, C16) allowed us to test whether the MINCLE-independent responses to TDM may not be caused by a specific propensity of the cord factor itself, but rather by more generic features of glycolipids. The results demonstrated a clear separation in the capacity of the glycolipids to induce inflammatory genes (e.g. *Csf3*) associated with MINCLE-dependent clusters 1 and 8 (Fig. 6), which required the diester form of C16, and the MINCLE-independent induction of genes associated with cluster 4 and 6 (Fig. 6), which was triggered also by the trehalose monoesters (which do not bind to MINCLE). This finding raises the question which alternative signaling mechanism(s) may be triggered by the cord factor and related glycolipids in macrophages. An obvious candidate is the close MINCLE relative MCL, which was identified as second cord factor receptor following the detection of residual transcriptional responses in *Mincle*^{-/-} mice (9) and can form heterodimers with MINCLE (66, 67). Although we have not tested whether MCL is responsible for kinase activation and gene expression in the absence of MINCLE in our system, we consider this unlikely for two reasons: first,

MINCLE-deficiency abrogates completely the activation of several canonical CLR pathway proteins (e.g. SYK, PKC δ ; ERK1/2) which would be shared by MCL signaling; second, the MINCLE-independent response appears to be functionally distinct based on the bioinformatic analysis of pathway and GO association of phosphoproteome and transcriptome changes. To confirm or reject this notion, MINCLE-independent phosphoprotein regulation and TDM target gene expression needs to be tested in macrophages treated with SYK-inhibitors and in FcR γ -deficient macrophages in future experiments. TLR/MYD88-dependent activation by the cord factor has been reported previously (12, 68), which could provide an alternative explanation for the MINCLE-independent signaling. Although we have not tested this possibility by using *Myd88*^{-/-} macrophages for analysis of MINCLE-independent target gene expression, the finding that pathway enrichment associated MYD88 signaling with the MINCLE-dependent response argues against this explanation. The scavenger receptors MARCO and MSR1 can also bind TDM (68); therefore, the phosphorylation of MSR1 prompted us to test its functional role in TDM-induced signaling and gene expression, but we did not observe differences in *Msr1*^{-/-} macrophages. Finally, our attempts to assign a role in MINCLE-independent target gene expression to two other candidate phosphoproteins, the complement receptor C5aR1 and the adapter protein FYB, were not successful. Activation of integrins by TDM may be another mechanism of MINCLE-independent signaling and is supported by phosphorylation of the kinases HCK and PTK2, both involved in integrin-signaling (69, 70). Importantly, receptor-independent mechanisms such as membrane alterations induced by TDM and related glycolipids encountered by macrophages should also be considered as potential cause of the MINCLE-independent phosphorylation events and transcriptional changes. Such direct interactions with membrane lipids and alterations in signaling molecule assembly have been described for urate acid crystals and aluminum hydroxide (71, 72).

Regardless of whether MINCLE-independent phosphorylation and transcriptional regulation are induced by receptor-independent membrane alterations or triggered by a specific receptor of yet unknown identity, the type of biological processes and pathway terms associated with it were remarkably distinct. Especially prominent was the association of cell cycle-related genes and phosphoproteins that included regulators of the DNA-damage response like the kinase ATR. In turn, the only significantly enriched kinase motif identified in the MINCLE-independent phosphosites was the ATM/ATR motif. The MINCLE-independent upregulation of several cyclins and the pro-proliferative transcription factors MYC and of the kinase CHEK1, by TDM correlated with increased cell density in macrophage cultures. Our observation that macrophage survival/growth is induced MINCLE-independently by several TDM-related glycolipids after 24h, but MINCLE-dependently further enhanced by the cord factor after 48h, suggests that

both pathways contribute to TDM-induced macrophage growth and survival. Phosphorylation of lamins, such as of LMNA observed here, contributes to regulation of the cell cycle (73). Thus, these data suggest that TDM promotes the survival and/or proliferation of macrophages and may thereby contribute to the dynamics of the granuloma response during mycobacterial infection. The concurrent activation of a DNA-damage response signature is at present unexplained but may be caused by the action of genotoxic substances like ROS and NO generated after stimulation with TDM, or could be a consequence of ATR activation because of replication stress. Recently, MYC-dependent DNA-damage response signaling was shown to be triggered in macrophages infected with *M. bovis* BCG, leading to the formation of multi-nucleated, polyploid macrophages through modified cell division (74). This pathway was MYD88-dependent and could be triggered by chronic stimulation with a bacterial lipopeptide TLR2 ligand (74). We have not determined whether the cell cycle/DNA-damage response observed here after TDM stimulation also leads to generation of multi-nucleated macrophages, but the similarity in the Myc-induction and ATM/ATR activity clearly suggests this possibility.

Taken together, we presented in this manuscript the first combined global analysis of the macrophage response to a C-type lectin receptor ligand at the phosphoproteome and transcriptome level. Our unbiased phosphoproteomic investigation of macrophage activation by the mycobacterial cord factor revealed many novel regulated phosphoproteins as components of MINCLE-dependent and -independent signaling, which appear to affect different biological processes and cellular components. The targeting of phagolysosomal and transport phosphoproteins by TDM-MINCLE signaling points to a role in the mycobacteria-macrophage interaction that merits further investigation. Likewise, the identification of robust AKT activation by TDM-MINCLE signaling and the essential role of p85 α -PI3K in this process and its downstream effects indicate an important role of this pathway in macrophage reprogramming during mycobacterial infection. The strong MINCLE-independent component of the global phosphorylation and transcriptional response was consistently characterized by alterations in cell cycle regulators and DNA-damage response genes. Although it remains to be clarified by which receptor and mechanism this MINCLE-independent TDM effect is brought about, it appears to constitute a significant aspect of macrophage reprogramming by the cord factor and resembles recently reported features of mycobacteria-induced macrophage phenotypical changes.

Acknowledgments—The authors thank Dr. Annegret Reinhold (Magdeburg, Germany) for providing bones of *Fyb*^{−/−} mice and Dr. Jörg Mages (It's Biology, Madrid, Spain) for support with RNAseq data analysis.

DATA AVAILABILITY

Mass spectrometric raw data and the MaxQuant outputs are available through the PRIDE repository (<https://www.ebi.ac.uk/pride/archive/>) (44) and have been assigned the identifier PXD009513. Individual MS/MS spectra of phosphopeptides can be found here: http://msviewer.ucsf.edu/prospector/cgi-bin/mssearch.cgi?report_title=MS-Viewer&search_key=dftfndgcpu&search_name=msviewer. RNAseq data sets have been submitted to Gene Expression Omnibus and will be available under accession number GSE115322.

* Work for this project in the Lang lab was funded by Deutsche Forschungsgemeinschaft (SFB 796, B06) and the IZKF of the Medical Faculty Erlangen (A69 to R.L.). The work in the Trost lab was funded by Medical Research Council UK (MC_UU_12016/5 to M.T.) and by the pharmaceutical companies supporting the Division of Signal Transduction Therapy Unit (Boehringer-Ingelheim, GSK and Merck KGaA, to M.T.). The work of M.B. was supported by the Federal Ministry of Education and Research (01EO1503) and the Deutsche Forschungsgemeinschaft (BO3482/3-3, BO3482/4-1).

§ This article contains **supplemental material**.

None of the authors has a competing commercial interest in relation to the submitted work.

‡‡‡ To whom correspondence should be addressed. E-mail: roland.lang@uk-erlangen.de.

Author contributions: M.H., M.T., and R.L. designed research; M.H., J.P., B.K., B.A., B.B., S.U., J.H., and C.B. performed research; M.H., B.K., B.A., J.H., C.B., A.B.E., M.T., and R.L. analyzed data; M.H., M.T., and R.L. wrote the paper; A.H., M.B., M.K., H.F., C.F., S.B.-H., and G.S. contributed new reagents/analytic tools.

REFERENCES

- Gopalakrishnan, A., and Salgame, P. (2016) Toll-like receptor 2 in host defense against *Mycobacterium tuberculosis*: to be or not to be—that is the question. *Curr. Opin. Immunol.* **42**, 76–82.
- Bafica, A., Scanga, C. A., Feng, C. G., Leifer, C., Cheever, A., and Sher, A. (2005) TLR9 regulates Th1 responses and cooperates with TLR2 in mediating optimal resistance to *Mycobacterium tuberculosis*. *J. Exp. Med.* **202**, 1715–1724.
- Tokunaga, T., Yamamoto, H., Shimada, S., Abe, H., Fukuda, T., Fujisawa, Y., Furutani, Y., Yano, O., Kataoka, T., Sudo, T., and et al. (1984) Antitumor activity of deoxyribonucleic acid fraction from *Mycobacterium bovis* BCG. I. Isolation, physicochemical characterization, and antitumor activity. *J. National Cancer Inst.* **72**, 955–962.
- Rothfuchs, A. G., Bafica, A., Feng, C. G., Egen, J. G., Williams, D. L., Brown, G. D., and Sher, A. (2007) Dectin-1 Interaction with *Mycobacterium tuberculosis* Leads to Enhanced IL-12p40 Production by Splenic Dendritic Cells. *J. Immunol.* **179**, 3463–3471.
- Yadav, M., and Schorey, J. S. (2006) The beta-glucan receptor dectin-1 functions together with TLR2 to mediate macrophage activation by mycobacteria. *Blood* **108**, 3168–3175.
- Yonekawa, A., Saijo, S., Hoshino, Y., Miyake, Y., Ishikawa, E., Suzukawa, M., Inoue, H., Tanaka, M., Yoneyama, M., Oh-Hora, M., Akashi, K., and Yamasaki, S. (2014) Dectin-2 is a direct receptor for mannose-capped lipoarabinomannan of mycobacteria. *Immunity* **41**, 402–413.
- Toyonaga, K., Torigoe, S., Motomura, Y., Kamichi, T., Hayashi, J. M., Morita, Y. S., Noguchi, N., Chuma, Y., Kiyohara, H., Matsuo, K., Tanaka, H., Nakagawa, Y., Sakuma, T., Ohmura, M., Yamamoto, T., Umemura, M., Matsuzaki, G., Yoshikai, Y., Yano, I., Miyamoto, T., and Yamasaki, S. (2016) C-type lectin receptor DCAR recognizes mycobacterial phosphatidyl-inositol mannosides to promote a Th1 response during infection. *Immunity* **45**, 1245–1257.
- Ishikawa, E., Ishikawa, T., Morita, Y. S., Toyonaga, K., Yamada, H., Takeuchi, O., Kinoshita, T., Akira, S., Yoshikai, Y., and Yamasaki, S. (2009) Direct recognition of the mycobacterial glycolipid, trehalose dimycolate, by C-type lectin Mincle. *J. Exp. Med.* **206**, 2879–2888.

9. Miyake, Y., Toyonaga, K., Mori, D., Kakuta, S., Hoshino, Y., Oyama, A., Yamada, H., Ono, K., Suyama, M., Iwakura, Y., Yoshikai, Y., and Yamasaki, S. (2013) C-type lectin MCL is an FcRgamma-coupled receptor that mediates the adjuvant activity of mycobacterial cord factor. *Immunity* **38**, 1050–1062
10. Schoenen, H., Bodendorfer, B., Hitchens, K., Manzanero, S., Werninghaus, K., Nimmerjahn, F., Agger, E. M., Stenger, S., Andersen, P., Ruland, J., Brown, G. D., Wells, C., and Lang, R. (2010) Cutting edge: Mincle is essential for recognition and adjuvant activity of the mycobacterial cord factor and its synthetic analog trehalose-dibehenate. *J. Immunol.* **184**, 2756–2760
11. Wilson, G. J., Marakalala, M. J., Hoving, J. C., van Laarhoven, A., Drummond, R. A., Kerscher, B., Keeton, R., van de Vosse, E., Ottenhoff, T. H., Plantinga, T. S., Alisjahbana, B., Govender, D., Besra, G. S., Netea, M. G., Reid, D. M., Willment, J. A., Jacobs, M., Yamasaki, S., van Crevel, R., and Brown, G. D. (2015) The C-type lectin receptor CLECSF8/CLEC4D is a key component of anti-mycobacterial immunity. *Cell Host Microbe* **17**, 252–259
12. Geisel, R. E., Sakamoto, K., Russell, D. G., and Rhoades, E. R. (2005) In vivo activity of released cell wall lipids of *Mycobacterium bovis* bacillus Calmette-Guerin is due principally to trehalose mycolates. *J. Immunol.* **174**, 5007–5015
13. Shenderov, K., Barber, D. L., Mayer-Barber, K. D., Gurcha, S. S., Jankovic, D., Feng, C. G., Oland, S., Hieny, S., Caspar, P., Yamasaki, S., Lin, X., Ting, J. P., Trinchieri, G., Besra, G. S., Cerundolo, V., and Sher, A. (2013) Cord factor and peptidoglycan recapitulate the Th17-promoting adjuvant activity of mycobacteria through mincle/CARD9 signaling and the inflammasome. *J. Immunol.* **190**, 5722–5730
14. Werninghaus, K., Babiak, A., Gross, O., Holscher, C., Dietrich, H., Agger, E. M., Mages, J., Mocsa, A., Schoenen, H., Finger, K., Nimmerjahn, F., Brown, G. D., Kirschning, C., Heit, A., Andersen, P., Wagner, H., Ruland, J., and Lang, R. (2009) Adjuvant activity of a synthetic cord factor analogue for subunit *Mycobacterium tuberculosis* vaccination requires FcRgamma-Syk-Card9-dependent innate immune activation. *J. Exp. Med.* **206**, 89–97
15. Desel, C., Werninghaus, K., Ritter, M., Jozefowski, K., Wenzel, J., Russkamp, N., Schleicher, U., Christensen, D., Wirtz, S., Kirschning, C., Agger, E. M., Prazeres da Costa, C., and Lang, R. (2013) The Mincle-activating adjuvant TDB induces MyD88-dependent Th1 and Th17 responses through IL-1R signaling. *PLoS ONE* **8**: e53531
16. Ostrop, J., and Lang, R. (2017) Contact, Collaboration, and Conflict: Signal integration of Syk-coupled C-type lectin receptors. *J. Immunol.* **198**, 1403–1414
17. LeibundGut-Landmann, S., O. Gross, M. J. Robinson, F. Osorio, E. C. Slack, S. V. Tsoni, E. Schweighoffer, V. Tybulewicz, G. D. Brown, J. Ruland, and C. Reis e Sousa. (2007) Syk- and CARD9-dependent coupling of innate immunity to the induction of T helper cells that produce interleukin 17. *Nat. Immunol.* **8**, 630–638
18. Bryant, C. E., Orr, S., Ferguson, B., Symmons, M. F., Boyle, J. P., and Monie, T. P. (2015) International Union of Basic and Clinical Pharmacology. XCIV. Pattern recognition receptors in health and disease. *Pharmacol. Rev.* **67**, 462–504
19. Sharma, K., Kumar, C., Keri, G., Breitkopf, S. B., Oppermann, F. S., and Daub, H. (2010) Quantitative analysis of kinase-proximal signaling in lipopolysaccharide-induced innate immune response. *J. Proteome Res.* **9**, 2539–2549
20. Sjoelund, V., Smelkinson, M., and Nita-Lazar, A. (2014) Phosphoproteome profiling of the macrophage response to different toll-like receptor ligands identifies differences in global phosphorylation dynamics. *J. Proteome Res.* **13**, 5185–5197
21. Weintz, G., Olsen, J. V., Fruhauf, K., Niedzielska, M., Amit, I., Jantsch, J., Mages, J., Frech, C., Dolken, L., Mann, M., and Lang, R. (2010) The phosphoproteome of toll-like receptor-activated macrophages. *Mol. Syst. Biol.* **6**, 371
22. Dambuzza, I. M., and Brown, G. D. (2015) C-type lectins in immunity: recent developments. *Curr. Opin. Immunol.* **32**, 21–27
23. Rogers, N. C., E. C. Slack, A. D. Edwards, M. A. Nolte, O. Schulz, E. Schweighoffer, D. L. Williams, S. Gordon, V. L. Tybulewicz, G. D. Brown, and C. Reis e Sousa. 2005. Syk-dependent cytokine induction by Dectin-1 reveals a novel pattern recognition pathway for C type lectins. *Immunity* **22**, 507–517
24. Strasser, D., Neumann, K., Bergmann, H., Marakalala, M. J., Guler, R., Rojowska, A., Hopfner, K. P., Brombacher, F., Urlaub, H., Baier, G., Brown, G. D., Leitges, M., and Ruland, J. (2012) Syk kinase-coupled C-type lectin receptors engage protein kinase C-sigma to elicit Card9 adaptor-mediated innate immunity. *Immunity* **36**, 32–42
25. Gross, O., Gewies, A., Finger, K., Schafer, M., Sparwasser, T., Peschel, C., Forster, I., and Ruland, J. (2006) Card9 controls a non-TLR signalling pathway for innate anti-fungal immunity. *Nature* **442**, 651–656
26. Goodridge, H. S., Simmons, R. M., and Underhill, D. M. (2007) Dectin-1 Stimulation by *Candida albicans* Yeast or Zymosan Triggers NFAT Activation in Macrophages and Dendritic Cells. *J. Immunol.* **178**, 3107–3115
27. Deribe, Y. L., Pawson, T., and Dikic, I. (2010) Post-translational modifications in signal integration. *Nat. Structural Mol. Biol.* **17**, 666–672
28. Fukao, T., Tanabe, M., Terauchi, Y., Ota, T., Matsuda, S., Asano, T., Kadowaki, T., Takeuchi, T., and Koyasu, S. (2002) PI3K-mediated negative feedback regulation of IL-12 production in DCs. *Nat. Immunol.* **3**, 875–881
29. Beer-Hammer, S., Zebidin, E., von Holleben, M., Alferink, J., Reis, B., Dressing, P., Grandi, D., Scheu, S., Hirsch, E., Sexl, V., Pfeffer, K., Nurnberg, B., and Piekorz, R. P. (2010) The catalytic PI3K isoforms p110gamma and p110delta contribute to B cell development and maintenance, transformation, and proliferation. *J. Leukoc. Biol.* **87**, 1083–1095
30. Kallerup, R. S., Madsen, C. M., Schioth, M. L., Franzky, H., Rose, F., Christensen, D., Korsholm, K. S., and Foged, C. (2015) Influence of trehalose 6,6'-diester (TDX) chain length on the physicochemical and immunopotentiating properties of DDA/TDX liposomes. *Eur. J. Pharmaceut. Biopharmaceut.* **90**, 80–89
31. Tyanova, S., Temu, T., Sinitcyn, P., Carlson, A., Hein, M. Y., Geiger, T., Mann, M., and Cox, J. (2016) The Perseus computational platform for comprehensive analysis of (prote)omics data. *Nat. Methods* **13**, 731–740
32. Boersema, P. J., Raijmakers, R., Lemeer, S., Mohammed, S., and Heck, A. J. (2009) Multiplex peptide stable isotope dimethyl labeling for quantitative proteomics. *Nat. Protoc.* **4**, 484–494
33. McNulty, D. E., and Annan, R. S. (2008) Hydrophilic interaction chromatography reduces the complexity of the phosphoproteome and improves global phosphopeptide isolation and detection. *Mol. Cell. Proteomics* **7**, 971–980
34. Thingholm, T. E., Jorgensen, T. J., Jensen, O. N., and Larsen, M. R. (2006) Highly selective enrichment of phosphorylated peptides using titanium dioxide. *Nat. Protoc.* **1**, 1929–1935
35. Lai, Y. C., Kondapalli, C., Lehneck, R., Procter, J. B., Dill, B. D., Woodroof, H. I., Gourlay, R., Pegg, M., Macartney, T. J., Corti, O., Corvol, J. C., Campbell, D. G., Itzen, A., Trost, M., and Muqit, M. M. (2015) Phosphoproteomic screening identifies Rab GTPases as novel downstream targets of PINK1. *EMBO J.* **34**, 2840–2861
36. Trost, M., English, L., Lemieux, S., Courcelles, M., Desjardins, M., and Thibault, P. (2009) The phagosomal proteome in interferon-gamma-activated macrophages. *Immunity* **30**, 143–154
37. Munoz, I. M., Morgan, M. E., Peltier, J., Weiland, F., Gregorczyk, M., Brown, F. C., Macartney, T., Toth, R., Trost, M., and Rouse, J. (2018) Phosphoproteomic screening identifies physiological substrates of the CDKL5 kinase. *EMBO J.* **37**, e99559
38. Cox, J., and Mann, M. (2008) MaxQuant enables high peptide identification rates, individualized p.p.b.-range mass accuracies and proteome-wide protein quantification. *Nat. Biotechnol.* **26**, 1367–1372
39. Dobin, A., Davis, C. A., Schlesinger, F., Drenkow, J., Zaleski, C., Jha, S., Batut, P., Chaisson, M., and Gingeras, T. R. (2013) STAR: ultrafast universal RNA-seq aligner. *Bioinformatics* **29**, 15–21
40. Patro, R., Duggal, G., Love, M. I., Irizarry, R. A., and Kingsford, C. (2017) Salmon provides fast and bias-aware quantification of transcript expression. *Nat. Methods* **14**, 417–419
41. Ritchie, M. E., Phipson, B., Wu, D., Hu, Y., Law, C. W., Shi, W., and Smyth, G. K. (2015) limma powers differential expression analyses for RNA-sequencing and microarray studies. *Nucleic Acids Res.* **43**, e47
42. Maere, S., Heymans, K., and Kuiper, M. (2005) BiNGO: a Cytoscape plugin to assess overrepresentation of gene ontology categories in biological networks. *Bioinformatics* **21**, 3448–3449
43. Rigbolt, K. T., Vanselow, J. T., and Blagoev, B. (2011) GProX, a user-friendly platform for bioinformatics analysis and visualization of quantitative proteomics data. *Mol. Cell. Proteomics* **10**, O110.007450

44. Vizcaino, J. A., Csordas, A., del-Toro, N., Dianas, J. A., Griss, J., Lavidas, I., Mayer, G., Perez-Riverol, Y., Reisinger, F., Ternent, T., Xu, Q. W., Wang, R., and Hermjakob, H. (2016) 2016 update of the PRIDE database and its related tools. *Nucleic Acids Res.* **44**, D447–D456
45. Schoenen, H., Huber, A., Sonda, N., Zimmermann, S., Jantsch, J., Lepenies, B., Bronte, V., and Lang, R. (2014) Differential control of Mincle-dependent cord factor recognition and macrophage responses by the transcription factors C/EBP β and HIF1 α . *J. Immunol.* **193**, 3664–3675
46. Yamasaki, S., Ishikawa, E., Sakuma, M., Hara, H., Ogata, K., and Saito, T. (2008) Mincle is an ITAM-coupled activating receptor that senses damaged cells. *Nat. Immunol.* **9**, 1179–1188
47. Oberstein, A., Perlman, D. H., Shenk, T., and Terry, L. J. (2015) Human cytomegalovirus pUL97 kinase induces global changes in the infected cell phosphoproteome. *Proteomics* **15**, 2006–2022
48. Steiger, J., Stephan, A., Inkeles, M. S., Realegeno, S., Bruns, H., Kroll, P., de Castro Kroner, J., Sommer, A., Batinica, M., Pitzler, L., Kalscheuer, R., Hartmann, P., Plum, G., Stenger, S., Pellegrini, M., Brachvogel, B., Modlin, R. L., and Fabri, M. (2016) Imatinib triggers phagolysosome acidification and antimicrobial activity against *Mycobacterium bovis* Bacille Calmette-Guérin in glucocorticoid-treated human macrophages. *J. Immunol.* **197**, 222–232
49. Zhang, F., Tao, Y., Zhang, Z., Guo, X., An, P., Shen, Y., Wu, Q., Yu, Y., and Wang, F. (2012) Metalloendopeptidase Steap3 coordinates the regulation of iron homeostasis and inflammatory responses. *Haematologica* **97**, 1826–1835
50. Wall, A. A., Luo, L., Hung, Y., Tong, S. J., Condon, N. D., Blumenthal, A., Sweet, M. J., and Stow, J. L. (2017) Small GTPase Rab8a-recruited phosphatidylinositol 3-kinase gamma regulates signaling and cytokine outputs from endosomal toll-like receptors. *J. Biol. Chem.* **292**, 4411–4422
51. Wevers, B. A., Kaptein, T. M., Zijlstra-Willems, E. M., Theelen, B., Boekhout, T., Geijtenbeek, T. B., and Gringhuis, S. I. (2014) Fungal engagement of the C-type lectin mincle suppresses dectin-1-induced antifungal immunity. *Cell Host Microbe* **15**, 494–505
52. Okkenhaug, K. (2013) Signaling by the phosphoinositide 3-kinase family in immune cells. *Annu. Rev. Immunol.* **31**, 675–704
53. Huber, A., Kallerup, R. S., Korsholm, K. S., Franzky, H., Lepenies, B., Christensen, D., Foged, C., and Lang, R. (2016) Trehalose diester glycolipids are superior to the monoesters in binding to Mincle, activation of macrophages in vitro and adjuvant activity in vivo. *Innate Immun.* **22**, 405–418
54. Caldon, C. E., and Musgrove, E. A. (2010) Distinct and redundant functions of cyclin E1 and cyclin E2 in development and cancer. *Cell Division* **5**, 2
55. Imperatore, F., Maurizio, J., Vargas Aguilar, S., Busch, C. J., Favret, J., Kowenz-Leutz, E., Cathou, W., Gentek, R., Perrin, P., Leutz, A., Berruyer, C., and Sieweke, M. H. (2017) SIRT1 regulates macrophage self-renewal. *EMBO J.* **36**, 2353–2372
56. Liu, L., Lu, Y., Martinez, J., Bi, Y., Lian, G., Wang, T., Milasta, S., Wang, J., Yang, M., Liu, G., Green, D. R., and Wang, R. (2016) Proinflammatory signal suppresses proliferation and shifts macrophage metabolism from Myc-dependent to HIF1 α -dependent. *Proc. Natl. Acad. Sci. U.S.A.* **113**, 1564–1569
57. Hastak, K., Paul, R. K., Agarwal, M. K., Thakur, V. S., Amin, A. R., Agrawal, S., Sramkoski, R. M., Jacobberger, J. W., Jackson, M. W., Stark, G. R., and Agarwal, M. L. (2008) DNA synthesis from unbalanced nucleotide pools causes limited DNA damage that triggers ATR-Chk1-dependent p53 activation. *Proc. Natl. Acad. Sci. U.S.A.* **105**, 6314–6319
58. Zhang, Q., Lee, W. B., Kang, J. S., Kim, L. K., and Kim, Y. J. (2018) Integrin CD11b negatively regulates Mincle-induced signaling via the Lyn-SIRP α -SHP1 complex. *Exp. Mol. Med.* **50**, e439
59. Lee, W. B., Yan, J. J., Kang, J. S., Zhang, Q., Choi, W. Y., Kim, L. K., and Kim, Y. J. (2017) Mincle activation enhances neutrophil migration and resistance to polymicrobial septic peritonitis. *Sci. Reports* **7**, 41106
60. Okkenhaug, K., Ali, K., and Vanhaesebroeck, B. (2007) Antigen receptor signalling: a distinctive role for the p110 δ isoform of PI3K. *Trends Immunol.* **28**, 80–87
61. Chaussade, C., Rewcastle, G. W., Kendall, J. D., Denny, W. A., Cho, K., Gronning, L. M., Chong, M. L., Anagnostou, S. H., Jackson, S. P., Daniele, N., and Shepherd, P. R. (2007) Evidence for functional redundancy of class IA PI3K isoforms in insulin signalling. *Biochem. J.* **404**, 449–458
62. Jan, W. C., Kao, M. C., Yang, C. H., Chang, Y. Y., and Huang, C. J. (2017) Phosphoinositide 3-kinase is involved in mediating the anti-inflammation effects of vasopressin. *Inflammation* **40**, 435–441
63. Luyendyk, J. P., Schabbauer, G. A., Tencati, M., Holscher, T., Pawlinski, R., and Mackman, N. (2008) Genetic analysis of the role of the PI3K-Akt pathway in lipopolysaccharide-induced cytokine and tissue factor gene expression in monocytes/macrophages. *J. Immunol.* **180**, 4218–4226
64. Bruns, H., Stegelmann, F., Fabri, M., Dohner, K., van Zandbergen, G., Wagner, M., Skinner, M., Modlin, R. L., and Stenger, S. (2012) Abelson tyrosine kinase controls phagosomal acidification required for killing of *Mycobacterium tuberculosis* in human macrophages. *J. Immunol.* **189**, 4069–4078
65. Lee, W. B., Kang, J. S., Choi, W. Y., Zhang, Q., Kim, C. H., Choi, U. Y., Kim-Ha, J., and Kim, Y. J. (2016) Mincle-mediated translational regulation is required for strong nitric oxide production and inflammation resolution. *Nat. Commun.* **7**, 11322
66. Lobato-Pascual, A., Saether, P. C., Fossum, S., Dissen, E., and Daws, M. R. (2013) Mincle, the receptor for mycobacterial cord factor, forms a functional receptor complex with MCL and Fc ϵ RI γ . *Eur. J. Immunol.* **43**, 3167–3174
67. Miyake, Y., Oh-Hora, M., and Yamasaki, S. (2015) C-type lectin receptor MCL facilitates Mincle expression and signaling through complex formation. *J. Immunol.* **194**, 5366–5374
68. Bowdish, D. M., Sakamoto, K., Kim, M. J., Kroos, M., Mukhopadhyay, S., Leifer, C. A., Tryggvason, K., Gordon, S., and Russell, D. G. (2009) MARCO, TLR2, and CD14 are required for macrophage cytokine responses to mycobacterial trehalose dimycolate and *Mycobacterium tuberculosis*. *PLoS Pathog.* **5**, e1000474
69. Lee, H. S., Moon, C., Lee, H. W., Park, E. M., Cho, M. S., and Kang, J. L. (2007) Src tyrosine kinases mediate activations of NF- κ B and integrin signal during lipopolysaccharide-induced acute lung injury. *J. Immunol.* **179**, 7001–7011
70. Suen, P. W., Ilic, D., Cavegion, E., Berton, G., Damsky, C. H., and Lowell, C. A. (1999) Impaired integrin-mediated signal transduction, altered cytoskeletal structure and reduced motility in Hck/Fgr deficient macrophages. *J. Cell Sci.* **112**, 4067–4078
71. Flach, T. L., Ng, G., Hari, A., Desrosiers, M. D., Zhang, P., Ward, S. M., Seamone, M. E., Vilaysane, A., Mucci, A. D., Fong, Y., Prenner, E., Ling, C. C., Tschoop, J., Muruve, D. A., Amrein, M. W., and Shi, Y. (2011) Alum interaction with dendritic cell membrane lipids is essential for its adjuvanticity. *Nat. Med.* **17**, 479–487
72. Ng, G., Sharma, K., Ward, S. M., Desrosiers, M. D., Stephens, L. A., Schoel, W. M., Li, T., Lowell, C. A., Ling, C. C., Amrein, M. W., and Shi, Y. (2008) Receptor-independent, direct membrane binding leads to cell-surface lipid sorting and Syk kinase activation in dendritic cells. *Immunity* **29**, 807–818
73. Torvaldson, E., Kochin, V., and Eriksson, J. E. (2015) Phosphorylation of lamins determine their structural properties and signaling functions. *Nucleus* **6**, 166–171
74. Hertwich, L., Nanda, I., Evangelou, K., Nikolova, T., Horn, V., Sagar Emy, D., Stefanowski, J., Rogell, L., Klein, C., Gharun, K., Follo, M., Seidl, M., Kremer, B., Munke, N., Senges, J., Fliegau, M., Aschman, T., Pfeifer, D., Sarrazin, S., Sieweke, M. H., Wagner, D., Dierks, C., Haaf, T., Ness, T., Zaiss, M. M., Voll, R. E., Deshmukh, S. D., Prinz, M., Goldmann, T., Holscher, C., Hauser, A. E., Lopez-Contreras, A. J., Grun, D., Gorgoulis, V., Diefenbach, A., Henneke, P., and Triantafyllidou, A. (2016) DNA Damage Signaling Instructs Polyloid Macrophage Fate in Granulomas. *Cell* **167**, 1264–1280.e1218